DOKUMEN BUKTI KORESPONDENSI ARTIKEL JURNAL

- Cover letter (Revision)
- Manuscript (Revision)
- Response to reviewers
- Manuscript (Edited and proofread)

Makassar, 18 October 2012

Dear Editor Electric Power System Research,

Please consider this revised paper for possible publication in your esteemed EPSR. Authors would like to mention that this is our original work and not being considered for publication elsewhere.

If you have any queries regarding this paper, please feel free to contact me.

Kind regards,

Ardiaty Arief
School of Electrical Engineering, Faculty of Engineering, Hasanuddin University
Email: aarief@ft.unhas.ac.id, ardiaty@engineer.com

Under Voltage Load Shedding in Power System with Wind Turbines Driven Doubly Fed Induction Generator

Ardiaty Arief[a,*], ZhaoYang Dong[b], Muhammad Bachtiar Nappu[a], Marcus Gallagher[c]

[a] Department of Electrical Engineering, University of Hasanuddin, Makassar SULSEL 90213, Indonesia

[b] EA Centre of Excellence of Intelligent Electricity Networks, University of Newcastle, Callaghan, NSW, 2308, Australia

[c] School of Information Technology and Electrical Engineering, University of Queensland, St Lucia, Brisbane, QLD 4072, Australia

ABSTRACT--This paper presents a design and implementation of a new method of under voltage load shedding in power system considering wind generators to maintain voltage stability following a severe disturbance. This design considers the dynamic modelling of load as well as dynamic model of wind turbines. This works demonstrates a method to determine minimum amount and the most appropriate location of load shedding. The proposed technique in this research involving an iterative algorithm based on trajectory sensitivity analysis to solve the load shedding problem. The amount of load to be shed for each iteration is set at small amount. Furthermore, trajectory sensitivity factor (TSF) at all load buses and aggregated wind generators buses are calculated to provide information about the bus that has the prevalent influence in enhancing the system stability. The bus with the highest TSF is then selected as the location of load shedding. This process is reiterated until the voltages at all buses are stable. Dynamic simulations are performed with the IEEE 14 bus Reliability Test System (RTS) as case study.

*Corresponding author: aarief@ft.unhas.ac.id, ardiaty@engineer.com

Keywords—doubly fed induction generator; trajectory sensitivity; under voltage load shedding; voltage stability; wind turbines.

1. Introduction

Distributed generations (DGs) have grown rapidly as a clean renewable energy alternative generation in the electricity industry due to their fast technological developments as well as their advantages in economic and environmental issues regarding to exhaustion fossil fuels from the conventional electricity generations and global warming problems [1-3]. In general, DG can be defined as the development electric power sources connected directly on the customer site of the meter or at the distribution system network [4]. Detailed definition, classification and benefits of DGs are provided in reference [5].

Wind energy generations is one of the most rapidly emergent DGs with the installed capacity in the world has exceeded 25 GW [6] and the yearly growth rate of 20% for the past few years [7]. Furthermore, in 2020 wind energy are estimated to contribute 12% of the world's electricity generation [8]. The most popular wind generator technology installed in the network nowadays is the wind turbine driven doubly fed induction generator (DFIG) [9]. DFIG is a variable speed machine but can provide power with constant voltage and frequency as its rotor speed fluctuates. Furthermore, when a bidirectional converter installed in the rotor, the range of rotor speed can be prolonged beyond the synchronous speed, hence the electrical power is produced from both the stator and the rotor [10]. DFIG has several advantages, such as variable speed operation to obtain maximum power extracted from the wind, adaptable power factor, better efficiency, ability to control reactive power without capacitive support and less converter rating [9, 11].

Nevertheless, because the DFIG stator is linked directly to the system and the limitation of excitation converter rating, DFIG can supply asynchronous power to the grid and rather responsive to disruptions [12]. When the power system is subjected to large disturbance, DFIG transfers decreased power to the system. The inequity between the mechanical and electrical power in the generator, speed up the wind turbine hence its speed becomes faster [13]. As the speed augmented, the DFIG then attracts more reactive power hence causing the system voltage drops. After the fault is cleared, the DFIG will be able to restore its normal operating condition only if the speed of the generator does not go over its critical speed [14].

The high penetration of wind power generation in the network will affect the system stability; especially the voltage stability hence various investigations on the effect of DFIG on system stability become the subject of intense research during the last few years [15-21]. One issue that did not receive much attention so far is load shedding in power system with wind generators. Under voltage load shedding (UVLS) plays a vital part in power system control when the system is subjected to large disturbances. Research has validated that UVLS is an effectual counter-measure deed against voltage collapse. With the enlargement of the integration of wind generation number into the network, there are requirement for the system operator to maintain the wind generators to keep supplying power to the system when the system voltage collapse rather than being disconnected [22]. Study in [23] proposes UVLS design in power system with DGs, but this study only uses static voltage analysis approach and does not consider the DG type. The drawback of such technique is it cannot clarify the dynamic nature of the voltage collapse incidents. Additionally, with the large installation of wind generators and other DGs, the dynamic behavior of the system after being perturbed will change substantially because of the different technologies of the DGs and conventional

generators [24].

In this paper, a novel analytical method is proposed to design a UVLS incorporating trajectory sensitivity analysis as a technique to determine amount and location for load shedding also observing the DFIG behavior after the system is being perturbed. The proposed method involves an iterative process that calculates the bus voltage trajectory sensitivities with respect of load shedding amount. At each step, the amount of load shedding is set to a small amount. In addition, a new formulation, namely Trajectory Sensitivity Factor (TSF) based on voltage trajectory sensitivities is employed to determine the load shedding location.

This paper is organized as follow. Section II describes the doubly fed induction generator technology. Section III elaborates the proposed method: trajectory sensitivity based UVLS design. Section IV gives the results and analysis and Section V concludes the main findings of the research. Findings of this research are expected to provide a better UVLS setting to confront the probability of voltage collapse incident, including in power system with DGs.

2. Doubly Fed Induction Generator Technology

2.1 DFIG Configuration

A DFIG is connected to the wind turbine through a gearbox and a back-to back voltage source converter [17]. The gearbox is essential to couple the rotor to the generator to control the speed ranges divergences between the rotor and generator. The stator winding of the DFIG and the other side of the converter that is supplying the rotor is connected to the power system. The voltage is kept at constant frequency whereas its magnitude is controlled by adjusting the generator stator flux. A typical configuration of a DFIG wind turbine

technology is shown schematically in Fig. 1. A more detailed explanation of the DFIG system can be found in [24-26]

2.2 DFIG Electrical Power Model for Dynamic Analysis

The mechanical power from the wind turbine is converted by the DFIG which is delivered to the system from both the stator and rotor windings [27]. Fig. 2 presents the equivalent circuit of a DFIG.

The voltage equations for the stator and rotor can be expressed by [27]

$$\overline{V_s} = V_s\angle 0^o = -R_s\,\overline{I_s} - jX_{ls}\,\overline{I_s} - jX_m\,\overline{I_s} - jX_m\,\overline{I_r} = -R_s\,\overline{I_s} - jX_s\,\overline{I_s} - jX_m\,\overline{I_r} \quad (1)$$

$$\frac{\overline{V_r}}{s} = -\frac{R_r}{s}\,\overline{I_r} - jX_{lr}\,\overline{I_r} - jX_m\,\overline{I_r} - jX_m\,\overline{I_s} = -\frac{R_r}{s}\,\overline{I_r} - jX_r\,\overline{I_r} - jX_m\,\overline{I_s} \quad (2)$$

where

$$X_s = X_{ls} + X_m \quad (3)$$

$$X_r = X_{lr} + X_m \quad (4)$$

$$s = \frac{(\omega_s - \omega_r)}{\omega_s} \quad (5)$$

The current of stator

$$\overline{I_s} = \frac{-\overline{V_s}(R_r + js\omega_s L_r) + \overline{V_r}(jX_m)}{\left(R_s R_r - sX_s X_r + sX_m{}^2\right) + j(R_r X_s + sR_s X_r)} \quad (6)$$

$$\overline{I_r} = \frac{\overline{V_s}(jsX_m) - \overline{V_r}(R_s + jX_s)}{\left(R_s R_r - sX_s X_r + sX_m{}^2\right) + j(R_r X_s + sR_s X_r)} \quad (7)$$

The active and reactive power at stator and rotor

$$P_s + jQ_s = 3\,\overline{V_s}\,\overline{I_s}^* \quad (8)$$

$$P_r + jQ_r = 3\,\overline{V_r}\,\overline{I_r}^* \quad (9)$$

The DFIG active power converted from mechanical power are the summation of the power between stator and rotor side and copper losses that can be express as

$$P_{DFIG} = P_s + P_r + P_s^{Loss} + P_r^{Loss} \quad (10)$$

$$P_s^{Loss} = I_s{}^2 R_s$$

$$P_r^{Loss} = {I_r}^2 R_r$$

$$P_{DFIG} = -3{I_r}^2 R_r \left(\frac{1-s}{s}\right) - 3\left(\frac{1-s}{s}\right) P_r = -3{I_r}^2 R_r \left(\frac{1-s}{s}\right) - 3\left(\frac{1-s}{s}\right) V_r\, I_r \cos(\varphi - \theta_r) \quad (11)$$

Where,

$\overline{V_s} = V_s \angle 0^{\circ}$ stator voltage;

$\overline{V_r} = V_r \angle \varphi$ rotor excitation voltage;

$\overline{I_s} = I_s \angle \theta_s$ stator current;

$\overline{I_r} = I_r \angle \theta_r$ rotor current;

$\bar{E}$ air gap voltage;

R_s and R_r stator and rotor resistance, respectively;

X_{ls} and X_{lr} stator leakage reactance and rotor leakage reactance, respectively;

X_m magnetization reactance;

X_s and X_r stator reactance and rotor reactance, respectively;

ω_s and ω_r stator synchronous speed and rotor speed, respectively;

s the slip;

P_s and Q_s stator active and reactive power, respectively;

P_r and Q_r rotor active and reactive power, respectively;

P_{DFIG} electrical power converted from mechanical power (total DFIG power);

P_s^{Loss} stator copper loss;

P_r^{Loss} rotor copper loss.

3. Trajectory Sensitivities Enhanced UVLS Scheme

3.1 Trajectory Sensitivity Analysis

Trajectory sensitivity analysis is a technique based on linearizing a system surrounding a certain trajectory and employs time domain simulations [28]. This technique computes the sensitivity of the dynamics relating to the constraints [29]. Trajectory sensitivity provides a method of enumerating changes in the system variables in connection with the quick changes of system parameters and initial conditions [30]. The basic methodology of trajectory

sensitivity computation of hybrid systems is illustrated in [30] as follow.

The systematical representation for voltage stability analysis of a power system is provided by the following differential-algebraic equation (DAE)

$$\dot{x} = f(x, y; \alpha) \tag{12}$$
$$0 = g(x, y; \alpha) \tag{13}$$

Where x is the vector of dynamic state variables; y is the vector of algebraic state variables such as load bus voltage magnitudes and angles; and α represents system parameters.

Trajectories of (12) and (13) illustrates the performance of the dynamic variables x and algebraic variables y, where flows of x and y can be defined, as

$$x(t) = \varphi_x(x_0, t, \alpha) \tag{14}$$
$$y(t) = \varphi_y(y_0, t, \alpha) \tag{15}$$

Sensitivities of the flows φ_x and φ_y to the initial conditions and parameter variations can be acquired by forming the Taylor series expansions of above equations, hence

$$\Delta x(t) = \Delta\varphi_x(x_0, t, \alpha) = \frac{\partial\varphi_x(x_0, t, \alpha)}{\partial\alpha}\Delta\alpha = \frac{\partial x(t)}{\partial\alpha}\Delta\alpha \cong x_\alpha(t)\Delta\alpha \tag{16}$$
$$\Delta y(t) = \Delta\varphi_y(y_0, t, \alpha) = \frac{\partial\varphi_y(y_0, t, \alpha)}{\partial\alpha}\Delta\alpha = \frac{\partial y(t)}{\partial\alpha}\Delta\alpha \cong y_\alpha(t)\Delta\alpha \tag{17}$$

An approximation based numerical method is used to compute the sensitivities x_α and y_α, consequently

$$x_\alpha = \frac{\partial x}{\partial\alpha} = \frac{\Delta x}{\Delta\alpha} \approx \frac{\varphi_x(x_0, t, \alpha + \Delta\alpha) - \varphi_x(x_0, t, \alpha)}{\Delta\alpha} \tag{18}$$
$$y_\alpha = \frac{\partial y}{\partial\alpha} = \frac{\Delta y}{\Delta\alpha} \approx \frac{\varphi_y(y_0, t, \alpha + \Delta\alpha) - \varphi_y(y_0, t, \alpha)}{\Delta\alpha} \tag{19}$$

The trajectory sensitivities from (17) and (19) are revised to meet the purpose of this study. The bus voltage magnitude and load shedding amount are both parameters represented by y

and α correspondingly, hence sensitivities of bus voltage variation after load shedding at any specified bus are computed can be defined as

$$\Delta V(t) = \Delta\varphi_V(V_0, t, P) = \frac{\partial\varphi_V(V_0, t, P)}{\partial P}\Delta P = \frac{\partial V(t)}{\partial P}\Delta P \cong V_P(t)\Delta P \tag{20}$$

$$\varphi V_P = \frac{\partial V}{\partial P} = \frac{\Delta V}{\Delta P} \approx \frac{\varphi_V(V_0, t, P + \Delta P) - \varphi_V(V_0, t, P)}{\Delta P} \tag{21}$$

3.2 Trajectory Sensitivity Factor

In addition, the trajectory sensitivities are performed to find the load shedding location. A trajectory sensitivity factor (TSF) is formulated to assess the contribution of bus *j* after load shedding to the system voltage stability. The sensitivities calculated are $[\partial V_i/\partial P_j]$, which inform the rate of change in voltage magnitude at bus *i* with respect to the load shedding amount variation at bus *j*. The TSF at bus *j* is computed by shedding active power at bus *j* by a small value then assessing its impact on voltage magnitudes at all critical buses along time domain. The TSF proposed in this work is defined as

$$TSF_j = TSF_j^{load} + TSF_j^{wind} \tag{22}$$

$$TSF_j^{load} = \sum_{i=1}^{n_k}\left[\sum_{t=0}^{t_s}\left[\frac{\partial \mathrm{V}_i^{load}}{\partial P_j}\right]_{t=t_k}\right] \tag{23}$$

$$TSF_j^{wind} = \sum_{i=1}^{n_{wind}}\left[\sum_{t=0}^{t_s}\left[\frac{\partial \mathrm{V}_i^{wind}}{\partial P_j}\right]_{t=t_k}\right] \tag{24}$$

$$\partial P_j = \Delta P_j = P_{shed_j}$$

Where,

P_{shed_j} load shedding amount at bus *j*

n_k number of critical buses

n_{wind} number aggregated DFIG buses

t_k time instant

t_s number of time instant

There are two components computed here: TSF_j^{load} and TSF_j^{wind}. TSF_j^{load} evaluates the voltage trajectory sensitivities at critical load buses with respect of load shedding at bus j, whereas TSF_j^{wind} assesses the voltage sensitivities at wind turbine buses with respect of load shedding at bus j. The bus with the highest TSF means that this bus has the largest effect on the voltage stability improvement of the critical buses hence will be selected as a candidate bus for location of UVLS. The flowchart of the proposed trajectory sensitivities based UVLS is shown in Fig. 3.

4. Simulation Results

4.1 Without DFIG Connected to the System

The proposed method is implemented at the IEEE 14 bus Reliability Test System. The system is assumed to be working on a stressed condition. The system load for this study is 511.36 MW that consists of 50% static load and 50% dynamic motor load. The detail of load modelling can be seen in [31]. In order to design the trajectory sensitivity based UVLS, a fault is applied between bus 6 and 13 then the fault is cleared by removing transmission line between bus 6 and 13. Firstly, we evaluate the UVLS design without any wind generator. Fig. 5(a) shows the voltage drop after disturbance. There are 5 critical buses which voltage collapse below the stability limit (0.9 pu). They are buses 9, 10, 12, 13 and 14 as shown in Fig. 5(b).

For this simulation, the load shedding amount is for each iteration set at approximately 1% of the total system load. In this case, we round the amount to 5 MW for each step. The trajectory sensitivity analysis is performed to assess the effect of load shedding of 5 MW at

each bus in the critical zone. Fig. 6(a) and Fig. 6(b) illustrate the voltage trajectory sensitivities of critical buses for the first iteration if load shedding is commenced at bus 14 and bus 6, respectively. From both of these figures, it can be concluded that the voltage trajectory sensitivities if load shedding at bus 14 are better than sensitivities at bus 6. Furthermore, TSF is calculated to provide a distinct indication for load shedding location. Here, we only compute the TSF_j^{load} since there are no wind generator yet. In computing the TSF_j^{load} value, we use time interval 0.5 second for period 0 – 20 second. Table 1 illustrates the TSF_j^{load} calculation for load shedding at buses 14 and 6.

Fig. 7 depicts the TSF value for each load bus at first iteration. As indicated in red bar, bus 14 has the highest TSF (1.854). Load shedding of 5 MW is simulated at bus 14 and the system voltage magnitude is re-evaluated. At this stage, the system is still unstable hence trajectory sensitivities are performed again to calculate the TSF. For this simulation, this process is repeated 6 times until the system voltages are stable (above 0.9 p.u.) and the results TSF calculation for each iteration and load shedding location based on the highest TSF are presented in Table 2 and Table 3, respectively. Hence, the load shedding locations are bus 14 and bus 13 with load shedding amount at each bus of 15 MW. The results of voltage improvement after load shedding of 30 MW at buses 14 and 13 can be seen in Fig. 8. It clearly proves that voltages at all buses improve significantly and the system stability is recovered.

4.2 With DFIG Connected to Bus 14

To evaluate the UVLS scheme with wind generators, we postulate aggregated DFIGs are connected to bus 14 with total accumulative power of 10 MW. The detail of the wind generators parameters are shown in Table 4.

Fig. 9(a) portrays the voltage behavior at all buses following disturbance between bus 6 and 13. Specifically, Fig 9(b) illustrates the voltage drop at critical buses, which there are only 3 buses, bus 12, 13 and 14.

In order to assess the effect of load shedding towards the critical load and DFIG buses, the trajectory sensitivity is carried out. Fig. 10(a) and Fig. 10(b) show the voltage trajectory sensitivities of critical buses for the first iteration if load shedding is undertaken at bus 14 and bus 13, correspondingly. It is clearly proven that the sensitivities if load shedding in bus 13 is superior than sensitivities if load shedding at bus 14. Additionally, by referring to Fig. 11, that presents the trajectory sensitivities of aggregated DFIGs voltage if load shedding at bus 14, 13 and 3. It also shows that by load shedding in bus 13, the voltage sensitivities of the DFIG bus are greater than sensitivities if load shedding at buses 14 or 3. Nevertheless, in order to decide a better quantitative conclusion, the TSF is calculated, where it is consisted of two components; the TSF_j^{load} and the TSF_j^{wind}. Similarly to the computation without DFIG, time interval used is also 0.5 second for period 0 – 20 second. TSF_j calculation for load shedding at buses 14, 13 and 3 is displayed in Table 5.

Fig. 12 conveys the results of TSF calculation at all load buses. Interestingly, bus 14 does not longer have the highest TSF. When aggregated DFIGs are connected to bus 14, bus 13 now has the largest TSF. Therefore, this bus has the biggest influence in improving the system stability. For this condition, the sensitivity analysis procedure is iterated 3 times, and the results of this process is expressed in Table 6. After load shedding with total amount of 15 MW (10 MW at bus 13 and 5 MW at bus 14), the system voltage recover to its stable condition where the result is portrayed in Fig. 13.

Fig. 14(a) and Fig. 14(b) illustrate the DFIG voltage drop and DFIG recovery after load shedding, respectively. Table 7 concludes the comparison of UVLS design with and without DFIG connected to system. It is obviously, that with wind generators integration to the system, the UVLS scheme changes and reduces the amount of load to be disengaged from the system.

5. Conclusions

This paper proposes a dynamic analysis based design of UVLS for stabilizing the system following disturbance and ensuring the system secure limits are satisfied. The design is based on trajectory sensitivities technique that calculates the sensitivity of the dynamics relating to the constraints and provides a method of enumerating changes in the system variables in connection with the quick changes of system parameters and initial conditions. In this paper, trajectory sensitivities are employed to determine the minimum amount of load shedding and to verify location of load shedding. Trajectory sensitivity factor (TSF) provides useful information to find the best location for load shedding. The bus with the highest TSF means that this bus has the largest effect to enhance the voltage stability of the critical buses hence will be selected as a candidate bus for location of UVLS.

This work simulates the system behavior after being perturbed with and without DFIG. From the simulations, the installation of DFIG can help the demand side management in critical situation by reducing the amount of load disconnected from the system. Before installation of DFIG, the amount of load shedding is 30 MW, whereas when DFIG is connected with total aggregated power 10 MW, the load shedding amount decreases to 15 MW.

The proposed method provides significant voltage improvement and by using the proposed method, various power system failures after the system being perturbed can be prevented, including in power system with wind generators. This method can be applied robustly with or without wind generator and can be applied considering other DG type as long as the DG unit is modeled accurately.

References

[1] T. Senjyu, Y. Miyazato, A. Yona, N. Urasaki, and T. Funabashi, "Optimal Distribution Voltage Control and Coordination with Distributed Generation," *IEEE Trans. Power Deliv.,* vol. 23, pp. 1236-1242, 2008.

[2] R. Caldon, A. Stocco, and R. Turri, "Feasibility of Adaptive Intentional Islanding Operation of Electric Utility Systems With Distributed Generation," *Electr. Power Syst. Res.,* vol. 78, pp. 2017-2023, 2008.

[3] A. Keane, Q. Zhou, J. W. Bialek, and M. O'Malley, "Planning and operating non-firm distributed generation," *IET Renew. Power Gener.,* vol. 3, pp. 455-464, 2009.

[4] T. Ackermann, G. Andersson, and L. Söder, "Distributed Generation: A Definition," *Electr. Power Syst. Res.,* vol. 57, pp. 195-204, 2001.

[5] W. El-Khattam and M. M. A. Salama, "Distributed Generation Technologies, Definitions and Benefits," *Electr. Power Syst. Res.,* vol. 71, pp. 119-128, 2004.

[6] J. B. Ekanayake, L. Holdsworth, W. XueGuang, and N. Jenkins, "Dynamic modeling of doubly fed induction generator wind turbines," *IEEE Trans. Power Syst.,* vol. 18, pp. 803-809, 2003.

[7] N. R. Ullah, T. Thiringer, and D. Karlsson, "Voltage and Transient Stability Support by Wind Farms Complying With the E.ON Netz Grid Code," *IEEE Trans. Power Syst.,* vol. 22, pp. 1647-1656, 2007.

[8] S. M. Muyeen, R. Takahashi, M. H. Ali, T. Murata, and J. Tamura, "Transient Stability Augmentation of Power System Including Wind Farms by Using ECS," *IEEE Trans. Power Syst.,* vol. 23, pp. 1179-1187, 2008.

[9] E. Vittal, M. O'Malley, and A. Keane, "A Steady-State Voltage Stability Analysis of Power Systems With High Penetrations of Wind," *IEEE Trans. Power Syst.,* vol. 25, pp. 433-442, 2010.

[10] R. Pena, J. C. Clare, and G. M. Asher, "A doubly fed induction generator using back-to-back PWM converters supplying an isolated load from a variable speed wind turbine," *IEE Proc. - Electr. Power Appl.,* vol. 143, pp. 380-387, 1996.

[11] N. Heng, S. Yipeng, Z. Peng, and H. Yikang, "Improved Direct Power Control of a Wind Turbine Driven Doubly Fed Induction Generator During Transient Grid Voltage Unbalance," *IEEE Trans. Energy Convers.,* vol. 26, pp. 976-986, 2011.

[12] Z. Peng, H. Yikang, and S. Dan, "Improved Direct Power Control of a DFIG-Based Wind Turbine During Network Unbalance," *IEEE Trans. Power Electron.,* vol. 24, pp. 2465-2474, 2009.

[13] A. Arulampalam, M. Barnes, N. Jenkins, and J. B. Ekanayake, "Power Quality and Stability Improvement of a Wind Farm Using STATCOM Supported with Hybrid Battery Energy Storage," *IEE Proc. Gener., Transm., Distrib.,* vol. 153, pp. 701-710, 2006.

[14] S. K. Salman and A. L. J. Teo, "Windmill Modelling Consideration and Factors Influencing the Stability of a Grid-Connected Wind Powerbased Embedded Generator," *IEEE Trans. Power Syst.,* vol. 18, pp. 793–802, 2003.

[15] V. Akhmatov and P. B. Eriksen, "A Large Wind Power System in Almost Island Operation; A Danish Case Study," *IEEE Trans. Power Syst.,* vol. 22, pp. 937-943, 2007.

[16] M. H. Ali and W. Bin, "Comparison of Stabilization Methods for Fixed-Speed Wind Generator Systems," *IEEE Trans. Power Deliv.,* vol. 25, pp. 323-331, 2010.

[17] C. Chompooinwai, C. Yingvivatanapong, K. Methaprayoon, and L. Wei-Jen, "Reactive Compensation Techniques to Improve the Ride-Through Capability of Wind Turbine During Disturbance," *IEEE Trans. Ind. Appl.,* vol. 41, pp. 666-672, 2005.

[18] M. J. Hossain, H. R. Pota, M. A. Mahmud, and R. A. Ramos, "Investigation of the Impacts of Large-Scale Wind Power Penetration on the Angle and Voltage Stability of Power Systems," *IEEE Syst. J.,* vol. PP, pp. 1-1, 2011.

[19] H. T. Le, S. Santoso, and T. Q. Nguyen, "Augmenting Wind Power Penetration and Grid Voltage Stability Limits Using ESS: Application Design, Sizing, and a Case Study," *IEEE Trans. Power Syst.,* vol. PP, pp. 1-1, 2011.

[20] U. Nayeem Rahmat and T. Torbjrn, "Variable Speed Wind Turbines for Power System Stability Enhancement," *IEEE Trans. Energy Convers.,* vol. 22, pp. 52-60, 2007.

[21] E. Vittal, M. O'Malley, and A. Keane, "Rotor Angle Stability With High Penetrations of Wind Generation," *IEEE Trans. Power Syst.,* vol. PP, pp. 1-1, 2011.

[22] W. Yi and X. Lie, "Coordinated Control of DFIG and FSIG-Based Wind Farms Under Unbalanced Grid Conditions," *IEEE Trans. Power Deliv.,* vol. 25, pp. 367-377, 2010.

[23] X. Ding and A. A. Girgis, "Optimal Load Shedding Strategy in Power Systems with Distributed Generation," in *IEEE Power Engineering Society Winter Meeting*, Columbus, Ohio, USA, January 28-31, 2001, pp. 788-793 vol.2.

[24] I. Erlich, J. Kretschmann, J. Fortmann, S. Mueller-Engelhardt, and H. Wrede, "Modeling of Wind Turbines Based on Doubly-Fed Induction Generators for Power System Stability Studies," *IEEE Trans. Power Syst.,* vol. 22, pp. 909-919, 2007.

[25] J. G. Slootweg, S. W. H. de Haan, H. Polinder, and W. L. Kling, "Modeling Wind Turbines in Power System Dynamics Simulations," in *IEEE Power Engineering Society Summer Meeting*, Vancouver, BC, Canada, July 15 - 19, 2001, pp. 22-26 vol.1.

[26] K. C. Divya and P. S. N. Rao, "Models for Wind Turbine Generating Systems and Their Application in Load Flow Studies," *Electr. Power Syst. Res.,* vol. 76, pp. 844-856, 2006.

[27] C.-H. Liu and Y.-Y. Hsu, "Effect of Rotor Excitation Voltage on Steady-State Stability and Maximum Output Power of a Doubly Fed Induction Generator," *IEEE Trans. Ind. Electron.,* vol. 58, pp. 1096-1109, 2011.

[28] K. N. Shubhanga and A. M. Kulkarni, "Determination of Effectiveness of Transient Stability Controls Using Reduced Number of Trajectory Sensitivity Computations," *IEEE Trans. Power Syst.,* vol. 19, pp. 473-482, 2004.

[29] J. Ma, D. Han, R.-M. He, Z.-Y. Dong, and D. J. Hill, "Reducing Identified Parameters of Measurement-Based Composite Load Model," *IEEE Trans. Power Syst.,* vol. 23, pp. 76-83, 2008.

[30] I. A. Hiskens and M. A. Pai, "Trajectory Sensitivity Analysis of Hybrid Systems," *IEEE Trans. Circuits Syst. I: Fundamental Theory and Appl.,* vol. 47, pp. 204-220, 2000.

[31] R. M. Rifaat, "On Composite Load Modeling for Voltage Stability and Under Voltage Load Shedding," in *IEEE Power Engineering Society General Meeting*, Denver, Colorado, USA, June 7 - 10, 2004, pp. 1603-1610 Vol.2.

Figure Captions

Tables and Figures

Table 1 TSF Calculation for Case without DFIG

	$\sum_{t=0}^{t_s}\left[\frac{\partial V_i^{load}}{\partial P_j}\right]_{t=t_k}$	
Bus j	14	6
Bus i		
9	0.271	0.037
10	0.223	-0.008
12	0.188	0.083
13	0.432	0.038
14	0.74	0.037
TSF_j^{load}	1.854	0.187

Table 2 TSF Value for Case without DFIG

	TSF Value					
Iteration	I	II	III	IV	V	VI
Bus Number						
2	0.205	0.134	0.110	0.098	0.074	0.026
3	0.211	0.167	0.149	0.106	0.079	0.034
4	0.398	0.302	0.257	0.211	0.086	0.057
5	0.342	0.264	0.216	0.174	0.123	0.089
6	0.187	0.112	0.098	0.077	0.056	0.034
9	0.978	0.849	0.798	0.731	0.674	0.324
10	1.125	1.046	0.987	0.923	0.879	0.585
11	1.302	1.213	1.168	1.092	1.021	0.793
12	1.324	1.265	1.205	1.158	1.115	0.967
13	1.743	1.419	**1.367**	1.257	**1.187**	**1.076**
14	**1.854**	**1.578**	1.319	**1.296**	1.159	1.025

Table 3 Load Shedding Locations for Case without DFIG

Iteration	Load Shedding Design	
	Location	Amount (MW)
I	Bus 14	5
II	Bus 14	5
III	Bus 13	5
IV	Bus 14	5
V	Bus 13	5
VI	Bus 13	5

Table 4 DFIG Parameters

Power rating	2 MVA
Voltage rating	13.8 kV
Frequency rating	60 Hz
Stator resistance (R_s)	0.01 pu
Stator reactance (X_s)	0.10 pu

Rotor resistance (R_r)	0.01 pu
Rotor reactance (X_r)	0.08 pu
Magnetization reactance (X_m)	3.00 pu
Inertia Constants	3 kWs/kVA

Table 5 TSF Calculation for Case Considering DFIG

Bus j	TSF_j^{load}	TSF_j^{wind}	TSF_j
3	0.0815	0.0365	0.118
13	2.054	0.812	2.866
14	0.851	0.658	1.509

Table 6 Load Shedding Locations for Case Considering DFIG

Iteration	Load Shedding Design	
	Location	Amount (MW)
I	Bus 13	5
II	Bus 13	5
III	Bus 14	5

Table 7 Comparison Load Shedding Scheme With and Without DFIG

	Load shedding Design		
	Location	Amount (MW)	Total (MW)
Without DFIG	Bus 14	15	30
	Bus 13	15	
With DFIG	Bus 13	10	15
	Bus 14	5	

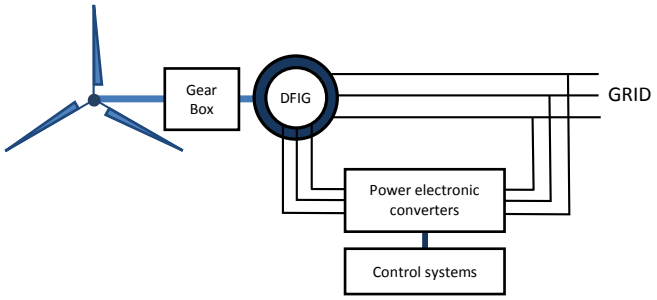

Fig. 1 DFIG wind turbine technology configuration

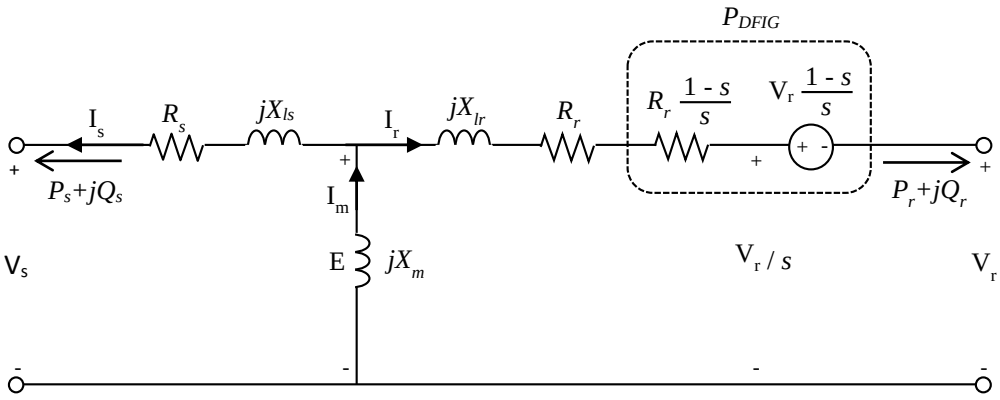

Fig. 2 DFIG equivalent circuit [27]

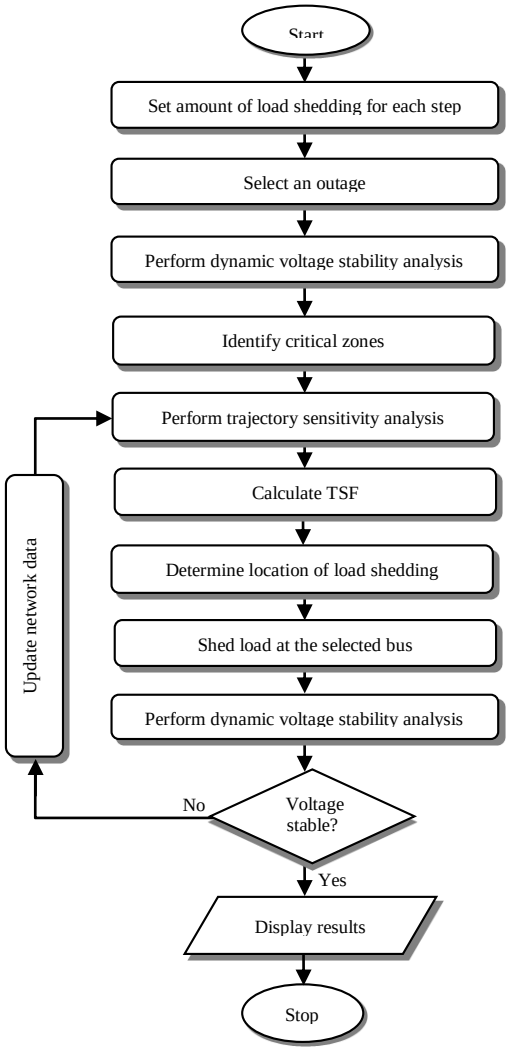

Fig. 3 Flowchart of the trajectory sensitivities based UVLS design

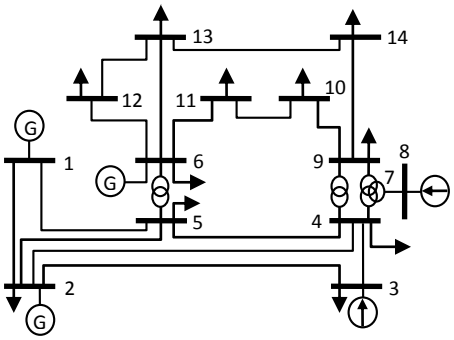

Fig. 4 The test system: IEEE 14 Bus Reliability Test System

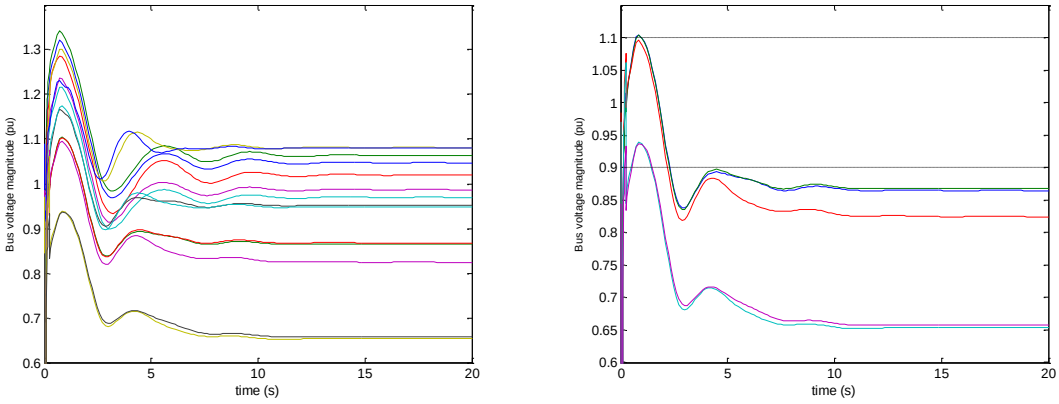

(a) at all buses (b) at the critical buses

Fig. 5 Voltage drop after outage between bus 6 and 13 without DFIG

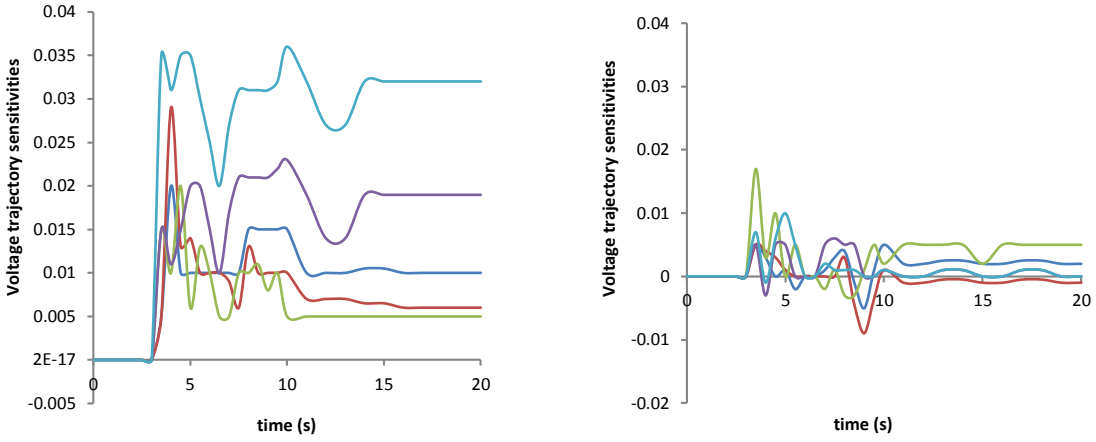

(a) at bus 14 (b) at bus 6

Fig. 6 Bus voltage trajectory sensitivities of critical buses if load shedding of 5 MW

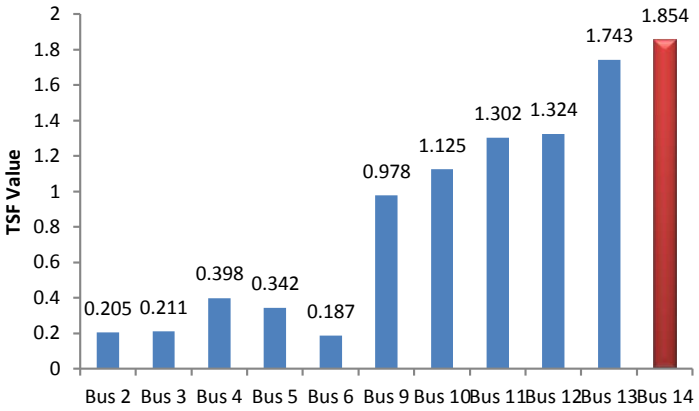

Fig. 7 TSF values at first iteration without DFIG

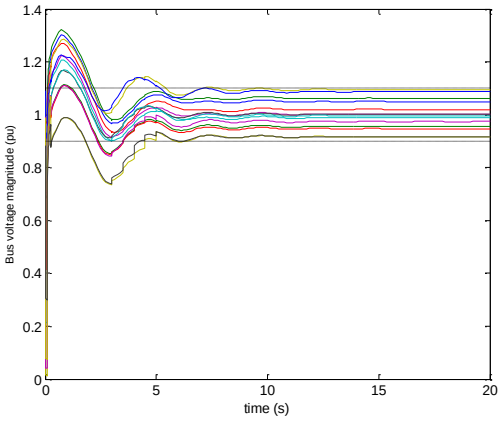

Fig. 8 Voltage profile improvement after load shedding without DFIG

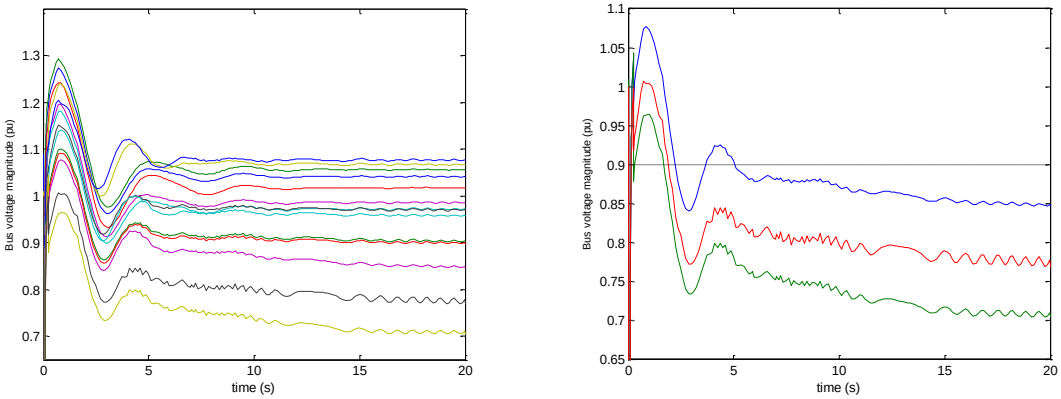

(a) at all load buses (b) at the critical buses

Fig. 9 Voltage drop after outage between bus 6 and 13 considering DFIG

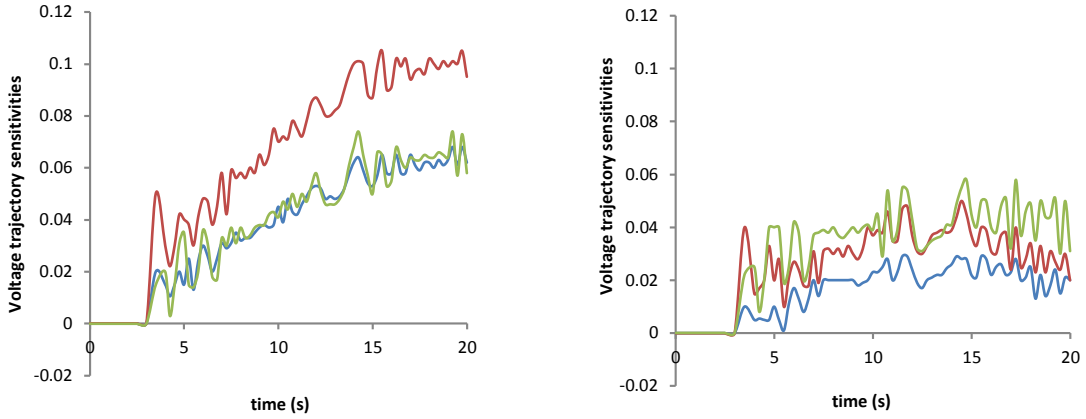

(a) at bus 13 (b) bus 14

Fig. 10 Bus voltage trajectory sensitivities of critical buses if load shedding of 5 MW

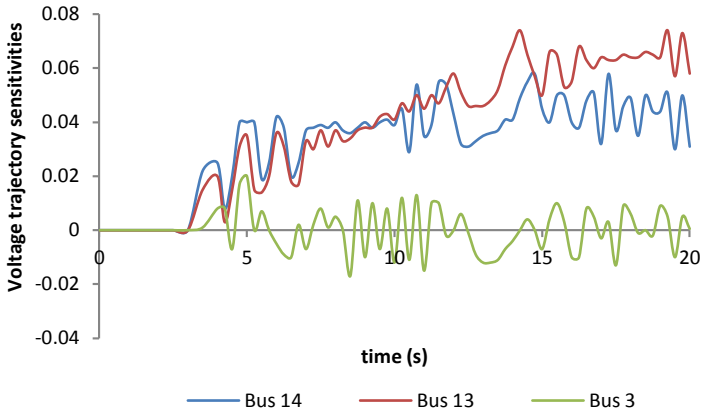

Fig. 11 DFIG voltage trajectory sensitivities load shedding of 5 MW applied at bus 14, 13 and 3

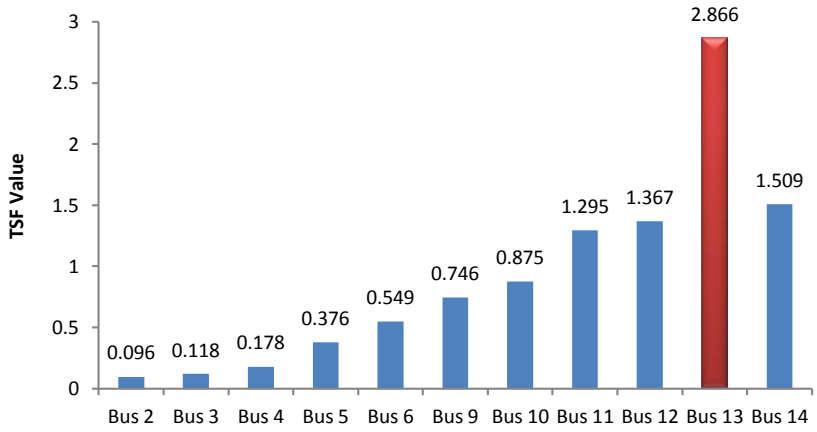

Fig. 12 TSF value at first iteration with DFIG

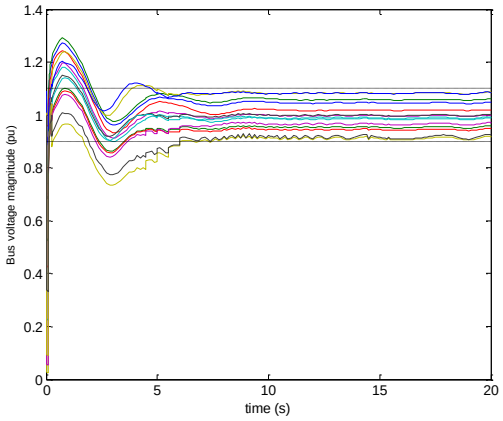

Fig. 13 Voltage profile improvement after load shedding with DFIG

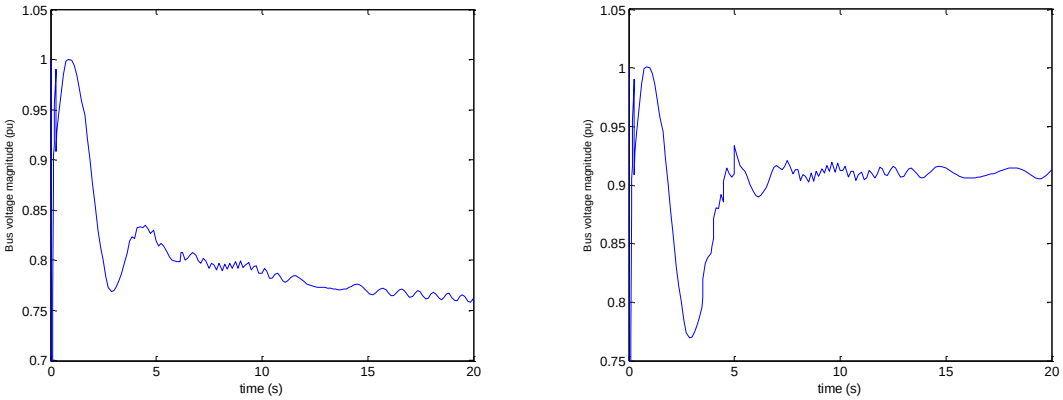

(a) voltage drop without load shedding (b) voltage improvement after load shedding

Fig. 14 Voltage behavior at DFIG bus

Authors would like to thank Editor and Reviewers. All the comments have been incorporated in the paper appropriately and below are the response to the reviewers' comments.

Reviewers' comments:

Reviewer #1: This paper presents a methodology to perform Under Voltage Load Shedding (UVLS) in power systems integrating Double Fed Induction Generators (DFIG) following severe system disturbances. The proposed methodology exploits trajectory sensitivity analysis to determine the most appropriate location of load shedding in each step (stage) of the UFLS scheme. This is a very useful aspect that will contribute to improve the performance of the UFLS strategy. However, these aspects should be put in context with the current state-of-the-art. In addition, several issues should be taken into account to improve the paper quality to an acceptable level suitable for publication. These issues are briefly described as follows:

1.The paper lacks a brief description regarding the fundamentals of UVLS and the available UVLS schemes. A critical overview regarding the application of UVLS schemes following the integration of DFIG is also missing. Under this context, the main challenges as well as the lack of solutions to deal with should be identified from the literature critical overview and the main contributions of this paper beyond the state-of-the-art should be properly highlighted.

Based on this suggestion, the authors have included fundamentals of UVLS and UVLS schemes. We also have mentioned the critical overview and the main contribution of this paper in the introduction. In this paper, a novel analytical method is proposed to design a UVLS incorporating trajectory sensitivity analysis as a technique to determine amount and location for load shedding also observing the DFIG behavior after the system is being perturbed. The proposed method involves an iterative process that calculates the bus voltage trajectory sensitivities with respect of load shedding amount. At each step, the amount of load shedding is set to a small amount. In addition, a new formulation, namely Trajectory Sensitivity Factor (TSF) based on voltage trajectory sensitivities is employed to determine the load shedding location.

2.The mathematical model representing the DFIG dynamic behavior is already well documented on the literature and therefore it is not essential to include its detailed description on this paper. Therefore, the Section 2 could be replaced by another one addressing the subjects mentioned previously, regarding UVLS.

We have replaced Section 2 with UVLS, as in suggestion no. 1.

3.Regarding the DFIG electrical model for dynamic analysis presented in Section 2.2 of this paper, the advanced control functionalities performed through the control systems of the back-to-back power electronic interface are missing. Also, many grid code requirements impose that DFIG provide Fault Ride Through and voltage control as system ancillary services. These features will impact on the system dynamic behavior following disturbances requiring the application of UVLS schemes to prevent voltage collapse and therefore on the design of suitable UVLS schemes and performance. Then, comments should be provided regarding these aspects. In addition, the main assumptions that were taken into account during the proposed UVLS scheme design should be presented and properly explained.

The authors have added a new section (Section 3) regarding control system used in the simulation.

4.The analysis of the results should consider the above mentioned features.

The analysis of the DFIG behavior is presented in Section 5.2.B.

5.Although the trajectory sensitivities subject does not belong to my domain of expertise, I suppose that a better explanation should be provided regarding the variables corresponding to voltage magnitude and load shedding amount represented by "y" and "alpha" in equations (17) and (19) and the sensitivities of bus voltage variations computed by equations (20) and (21).

In the Section 4.1, we have provided explanation as follow:
The systematical representation for voltage stability analysis of a power system is provided by the following differential-algebraic equation (DAE)

$$\dot{x} = f(x, y; \alpha) \quad (9)$$

$$0 = g(x, y; \alpha) \quad (10)$$

Where x is the vector of dynamic state variables; y is the vector of algebraic state variables such as load bus voltage magnitudes and angles; and α represents system parameters, such as power. In this study α is the amount of load shedding. Therefore, the trajectory sensitivities from (14) and (16) (new equation number) are revised by replacing y with bus voltage magnitude and α with load shedding amount, hence we obtain equations (17) and (18).

6.The implementation of load shedding strategies aims to shed the minimum amount of load to prevent voltage collapse in the system under study. Therefore, the adopted UVLS scheme should be presented in the paper together with the procedure used to compute the minimum amount of load to be shed (in each stage).

The algorithm and the flowchart (Fig. 5) are given in pages 12 and 13, respectively.

7.Some comments should also be provided regarding the computational time required to perform each iteration and the impact of the corresponding delay on the UVLS

effectiveness. On the other hand, it was supposed that representative contingencies are selected to design the UVLS scheme. Comments should be provided regarding these previous aspects.

In this work, the dynamic simulation for each iteration varies between 15 – 30 seconds. We have added information in the paper, that the outage was a critical outage and chosen based on a contingency analysis. This method is performed off-line, to give guidance for load shedding at real time, hence not causing delay in real time operation.

8.How representative are the simulated contingencies to conclude about the effectiveness of the proposed UVLS scheme? Additional comments are required regarding this subject.

Prior to designing the UVLS scheme, contingency analysis is performed to choose the critical outage. Based on this analysis, the outage between bus 6 and bus 13 is chosen as case study. Because there are significant voltages drop in some buses and need load shedding. However, not all outage will need load shedding. For example, outage between bus 13 and 14, because of this outage the system voltage can recover back to its stable condition, hence no load shedding is needed. In our study, we simulated if outage at main transmission line, for example: between buses 6-12, 12-13, 6-11, 9-10,or 9-14 and the load shedding scheme is the same.

9.Although without DFIG, a similar work was reported previously by the authors in the following paper titled as "Under voltage load shedding utilizing trajectory sensitivity to enhance voltage stability", AUPEC, 2011, which was not included on the list of references of this paper. Then, regarding this previous work, the innovative aspects and additional contributions should be properly highlighted.

This previous work in AUPEC 2011 only simulated without considering of any DG in the system and it evaluates the system with static load modelling only. In this journal paper is more detailed the UVLS design that compute the amount and location for load shedding and considering dynamic load modelling, whereas in the previous work only consider static load model. Which based on our simulations, load modelling with only static model gives different result hence may give biased

10.Additional important references regarding UVLS should be included, such as: [1] Ladhani, S.S.; Rosehart, W., Under voltage load shedding for voltage stability overview of concepts and principles, IEEE Power Engineering Society General Meeting, 2004; [2] S. Imai, Undervoltage Load Shedding Improving Security as Reasonable Measure for Extreme Contingencies. IEEE PES Transactions on Power Delivery; [3] IEEE Power System Relaying Committee Report, Summary of System Protection and Voltage Stability, Transactions on Power Delivery, Vol. 10. No. 2, April 1995; [4] Undervoltage Load Shedding Task Force (UVLSTF), Technical Studies Subcommittee of the WECC, Undervoltage Load Shedding Guidelines, July 1999.

Based on this suggestion, we have included them in the references.

11.The written English should be improved in order to make easier both the paper reading and understanding.

The paper has been proofread.

Reviewer #2: 1. The English requires revision from behalf of the authors. To give some examples:
* the term "generation" is used instead of "generator" when referring to the actual machine. E.g. in the introduction "Distributed generations", "Wind energy generations"
* sometimes the verb is used in its 3rd person plural form instead of 3rd person singular and vice-versa. E.g., in the second paragraph of Introduction "wind energy are estimated to contribute .."
* the use of strange terms like "asynchronous power" (first row page 3)
* some phrases in the introduction are difficult to comprehend. E.g. the second paragraph of the Introduction.

The paper has been proofread.

2. Other content comments:
* Page 7: it is said that equations (12) -(13) are the "systematical representation" of the power system for voltage stability. Is not complete, as such a representation is used to generally express the dynamics of the PS (or, more general, of any non linear system)

Thank you for your comment. We have corrected this is that these equations are systematic representation of a power system in general which can be applied in voltage stability analysis, where we have provided explanation that x is the vector of dynamic state variables; y is the vector of algebraic state variables such as load bus voltage magnitudes and angles; and α represents system parameters, such as power. In this study α is the amount of load shedding.

* Page 7-8: it is not clear how the sensitivities are really computed because the notation adopted for equation (20) is not coherent with the previous equations.

In the Section 4.1, we have provided explanation as follow:
The systematical representation for voltage stability analysis of a power system is provided by the following differential-algebraic equation (DAE)

$$\dot{x} = f(x, y; \alpha) \tag{9}$$

$$0 = g(x, y; \alpha) \quad (10)$$

Where x is the vector of dynamic state variables; y is the vector of algebraic state variables such as load bus voltage magnitudes and angles; and α represents system parameters, such as power. In this study α is the amount of load shedding. Therefore, the trajectory sensitivities from (14) and (16) (new equation number) are revised by replacing y with bus voltage magnitude and α with load shedding amount, hence we obtain equations (17) and (18).

3. Some observations in what regards the simulations:
* the time-domain figures do not specify which curves represent which buses. Is hard to read them.

We have specified the buses represented by the curves in Figs. 7(b), 8, 11(b), 12, and 13.

* In the case with DFIG in service, 10 MW of WG are introduced. But, the total generation in the system is ?510 MW. So, only 2% of generation is WG; is this relevant for a system where the WG penetration level should be high (as said in the introduction)?

For the aim of this research, we have performed several simulations. When the wind generation is more, then with the same fault there will be no load shedding needed, because the system can still recover back to its stability. Perhaps with bigger and more complex system, the DFIG percentage can be bigger but still achieving the objective of the research.

* Page 10: the location of the shedding is made according to the TSF which is computed using the voltage trajectory sensitivities. In this regard, the presentation of the results is a little bit confusing. It first presents the trajectory sensitivities of load shed at 2 buses, and one is better. Then it results that one of them has the highest TSF while the other one a low TSF. In my opinion a better analysis would be to first present the TSF values and compare, in terms of trajectory sensitivities, the bus with the best TSF with the others with the purpose to understand why the bus with the best TSF is indeed the best. Therefore, it is interesting to analyze this scenario: in case that difference of TSF in two different busses is little (for example, busses 13 and 14 of figure 7), what is the effect of the load shedding if it is applied to these two busses. In other words, it is necessary to show the relation between the order given by TSF and voltage answer.

The results presentation is based on the step taken in the study. Firstly, we analysis the voltage trajectory sensitivity each buses, which in this paper we presented 2 buses. It clearly shows the one with wider sensitivity, show that by performing load shedding in this particular bus will give significant voltage improvement. Then for a quantitative result we calculate the TSF which the results of TSF at all load buses are represented. Because we want to find the location for load shedding, therefore we simulated the trajectory sensitivity

considering load shedding of small amount (1% or approximately 5 MW), then we do it again until the system can recover back to its stability condition. Values of TSF provide information accumulative of the impact of load shedding at that bus to improve the voltage level at all critical buses.

* It is not clear if the lower shed quantity in the second simulation case is due to the characteristics of DFIG. Adding any kind of extra generation should improve the controllability and hence positively impact the load shedding. In this regard: was the DFIG set to control the voltage at its busbar? Do the DFIGs work at constant power factor? Generally, the impact of the DFIG should be discussed more in details.

The lower quantity of load shedding is affected by various effects and one of it is the installation of distributed generation (DG). DG can reduce power flow in the network hence reducing losses because DG in general provides electricity directly to the system. But as explained in the introduction, the UVLS design must robust so that the voltage at DFIG bus can recover. We have discussed the impact of DFIG installation in Section 5.2.B and we assessed if load shedding is performed at bus 3 that has low TSF. Based on our simulations, when we perform load shedding at bus with low TSF, the voltage at the DFIG bus cannot recover.

* Finally, the figure 5 shows the voltage values after the outage of line 6-13. Looking at the figure, a strong variation of the voltages is evident. To understand the numerical results some details about the values of the load at bus 13, the load factor of line 6-13 and the characteristics of AVR adopted for the generating units are necessary.

Based on this suggestion, the authors have added a new section (Section 3) regarding control system, including AVR used in the simulation. This study is based on dynamic analysis. However, from the static report, we obtained the load factor of line 6-13 = 38.295% whereas the load at bus 13 is 0.47 + j 0.18916 p.u.

AUTHOR QUERY FORM

ELSEVIER	**Journal:** EPSR **Article Number:** 3623	**Please e-mail or fax your responses and any corrections to:** **E-mail:** corrections.esch@elsevier.thomsondigital.com **Fax:** +353 6170 9272

Dear Author,

Please check your proof carefully and mark all corrections at the appropriate place in the proof (e.g., by using on-screen annotation in the PDF file) or compile them in a separate list. Note: if you opt to annotate the file with software other than Adobe Reader then please also highlight the appropriate place in the PDF file. To ensure fast publication of your paper please return your corrections within 48 hours.

For correction or revision of any artwork, please consult http://www.elsevier.com/artworkinstructions.

Any queries or remarks that have arisen during the processing of your manuscript are listed below and highlighted by flags in the proof. Click on the 'Q' link to go to the location in the proof.

Location in article	Query / Remark: **click on the Q link to go** **Please insert your reply or correction at the corresponding line in the proof**
Q1	Please confirm that given names and surnames have been identified correctly.
Q2	Please check affiliations for correctness.
Q3	Please check the placement of Figs. 6 and 16, and correct if necessary.
Q4	Fig. 8 will appear in black and white in print and in color on the web. Based on this, the figure caption has been updated. Please check, and correct if necessary.
	Please check this box if you have no corrections to make to the PDF file ☐

Thank you for your assistance.

Electric Power Systems Research xx (2012) xxx–xxx

Contents lists available at SciVerse ScienceDirect

Electric Power Systems Research

journal homepage: www.elsevier.com/locate/epsr

Highlights

Electric Power Systems Research xx (2012) xxx–xxx

Under voltage load shedding in power systems with wind turbine-driven doubly fed induction generators

Ardiaty Arief*, ZhaoYang Dong, Muhammad Bachtiar Nappu, Marcus Gallagher

- New method of under voltage load shedding considering wind generators is proposed.
- The technique employs trajectory sensitivity analysis involving iterative algorithm.
- We formulate trajectory sensitivity factor to find load shedding location.
- Various power system failures after the system being perturbed can be prevented.
- This scheme can be applied robustly with or without wind generator or other DG type.

Electric Power Systems Research xxx (2012) xxx–xxx

Contents lists available at SciVerse ScienceDirect

Electric Power Systems Research

journal homepage: www.elsevier.com/locate/epsr

Under voltage load shedding in power systems with wind turbine-driven doubly fed induction generators

Q1 Ardiaty Arief[a,*], ZhaoYang Dong[b], Muhammad Bachtiar Nappu[c], Marcus Gallagher[c]

Q2 [a] Department of Electrical Engineering, University of Hasanuddin, Makassar 90213, Indonesia
[b] EA Centre of Excellence of Intelligent Electricity Networks, University of Newcastle, NSW, Australia
[c] School of Information Technology and Electrical Engineering, University of Queensland, ~~Brisbane,~~ St Lucia, QLD 4072, Australia

ARTICLE INFO

Article history:
Received 21 March 2012
Received in revised form 18 October 2012
Accepted 25 October 2012
Available online xxx

Keywords:
Doubly fed induction generator
Trajectory sensitivity
Under voltage load shedding
Voltage stability
Wind turbines

ABSTRACT

This paper presents the design and implementation of a new method of under voltage load shedding in a power system incorporating the use of wind generators to maintain voltage stability following a severe disturbance. This design considers the dynamic modeling of the load as well as the dynamic model of wind turbines. This work demonstrates a method to determine the minimum amount and the most appropriate location of load shedding. The proposed technique in this research involves an iterative algorithm based on trajectory sensitivity analysis to solve the load shedding problem. The load to be shed for each iteration is set at a small amount. Furthermore, the trajectory sensitivity factor (TSF) at all load buses and aggregated wind generator buses are calculated to provide information about the bus that has the prevalent influence in enhancing the system stability. The bus with the highest TSF is then selected as the location of the load shedding. This process is reiterated until the voltages at all buses are stable. Dynamic simulations are performed with the IEEE 14 bus Reliability Test System as a case study.

1. Introduction

The most popular wind generator technology installed in the power networks nowadays is the wind turbine-driven doubly fed induction generator (DFIG). The DFIG is a variable speed machine but can provide power with constant voltage and frequency as its rotor speed fluctuates. Furthermore, when a bidirectional converter is installed in the rotor, the range of rotor speed can be prolonged beyond the synchronous speed; hence, the electrical power is produced from both the stator and the rotor [1]. The DFIG has several advantages, such as a variable speed operation to obtain the maximum power extracted from the wind, adaptable power factor, better efficiency, ability to control the reactive power without capacitive support and less converter rating [2,3].

The high penetration of wind power generation in the network will affect the system's stability, especially the voltage stability; hence, the effect of the DFIG on system stability has become the subject of intense research during the past few years [4–10]. One issue that has not received much attention so far is load shedding in a power system with wind generators. Under voltage load shedding (UVLS) plays a vital part in power system control when the system is subjected to large disturbances. Research has validated that UVLS is an effectual counter-measure against voltage collapse. With the integration of large numbers of wind generators into the network, there is a requirement for the system operator to maintain the wind generators to keep supplying power to the system when the system voltage collapse occurs rather than being disconnected [11]. Nevertheless, because the DFIG stator is linked directly to the system and the limitation of excitation converter ratings, the DFIG can supply asynchronous power to the grid and be rather responsive to disruptions [12]. When the power system is subjected to a large disturbance, the DFIG transfers decreases power to the system. The inequity between the mechanical and electrical power in the generator speeds up the wind turbine; hence, its speed becomes faster [13]. As the speed is augmented, the DFIG then attracts more reactive power hence causing the system voltage to drop. After the fault is cleared, the DFIG is able to restore its normal operating condition only if the speed of the generator does not go over its critical speed [14]. Therefore, in a UVLS design this issue must be considered, so that the UVLS scheme can ensure that the DFIG can restore its normal operating condition and the system voltage can recover back to its stability limit.

The study in [15] proposes a UVLS design in a power system with distributed generations (DG), but this study only uses the static voltage analysis approach and does not consider the DG type. The drawback of such a technique is it cannot clarify the dynamic nature of the voltage collapse incidents. Additionally, with the widespread installation of wind generators and other DGs, the

* Corresponding author. Tel.: +62 812 41 693 693.
E-mail addresses: aarief@ft.unhas.ac.id, ardiaty@engineer.com (A. Arief), zydong@ieee.org (Z. Dong), bachtiar@ieee.org (M.B. Nappu), marcusg@itee.uq.edu.au (M. Gallagher).

0378-7796/$ – see front matter © 2012 Elsevier B.V. All rights reserved.
http://dx.doi.org/10.1016/j.epsr.2012.10.013

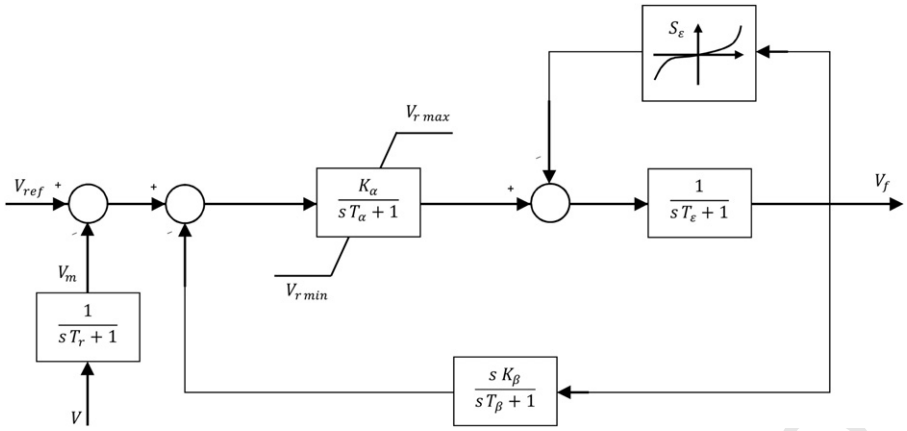

Fig. 1. Standard IEEE AVR type 1 excitation system model [24].

dynamic behavior of the system will change substantially after being perturbed because of the different technologies of the DGs and conventional generators [16].

In this paper, a novel analytical method is proposed to design a UVLS incorporating trajectory sensitivity analysis as a technique to determine the amount and location for load shedding and also observing the DFIG behavior after the system has been perturbed. The proposed method involves an iterative process that calculates the bus voltage trajectory sensitivities with respect to the load-shedding amount. At each step, the load shedding is set to a small amount. In addition, a new formulation, namely, the trajectory sensitivity factor (TSF) based on voltage trajectory sensitivities is employed to determine the load shedding location.

This paper is organized as follows. Section 2 provides an overview of the fundamental principles and current schemes of UVLS. Section 3 provides the details of a control system which is an automatic voltage and DFIG control system. Section 4 elaborates the proposed method for the trajectory sensitivity-based UVLS design. Section 5 gives the results and analysis, and Section 6 concludes the main findings of the research.

2. Power system under voltage load shedding

UVLS is an economical option to maintain voltage stability while waiting for the completion of new generation or transmission line projects [17]. Many utilities around the world have applied UVLS schemes. Imai [18] provided examples of existing UVLS applications in some utilities with their specific setting. The philosophy of UVLS is that whenever the system is disrupted, leading to voltage drop conditions below a certain pre-selected level for a certain predetermined time period, then selected loads should be removed [19]. It is expected that the system voltage will be restored to its normal limit by cutting off some loads. The objective of a UVLS is to reinstate the balance power within the system, to avert voltage collapse and to manage the voltage problems residing within a local area rather than permitting the problem to spread out to other areas [20]. The design of a load shedding should be "robust". UVLS must cover enough loads and must not be overly sensitive. Therefore, there are some considerations to ensure efficient load shedding as follows [19,21]:

- *Determination of amount of load to be shed*: Shedding an adequate amount of load is imperative in order to ensure UVLS can mitigate the menace of voltage instability. Shedding an insufficient amount of the necessary load will not be effective in arresting voltage collapse; on the other hand, shedding more load than required may lead to an over frequency circumstance.
- *Selection of location of load to be shed*: The study in [22] shows that shedding load in the correct location can arrest voltage instability. However, shedding the same amount of load in a different location gives a different result and may not be effective to improve the system stability.
- *Determination of timing and time steps of load shedding*: Load shedding is executed in steps in order to preclude the condition of over shedding. The minimum time delay before UVLS is triggered should be sufficient to prevent voltage collapse as well as to avoid unnecessary tripping during the transient time where load shedding is unnecessary.

Currently, there are two UVLS schemes being installed: decentralized (or distributed) UVLS, and centralized UVLS [19]. In both types, under voltage relays are set up at primary distribution substations which are near to major transmission substations to gauge the voltage at the transmission system. The decentralized system has better reliability than the centralized system because of its diversification. Failure of one element will not destructively intrude on the operation of other load shedding components. Load shedding in this scheme is concentrated to definite areas where the instability consequences are felt most sturdily. However, in a centralized scheme, under voltage appraising relays are sited at the most appropriate location in the system, not constrained to be close to a suitable load. The system voltages are observed at chosen strategic locations, which are usually the vital supply buses. In these crucial buses, the voltage level is securely controlled under the usual setting. In this structure, a verdict to execute load shedding is taken after significant low voltages transpire throughout the system by means of communications between primary localities.

3. Automatic voltage regulator and DFIG control system

3.1. Automatic voltage regulator

Modern generators are prepared with an automatic voltage regulator (AVR). An AVR outlines the primary voltage regulation of the generator and its function is to sustain the constant terminal voltage and to monitor the reactive power output [23]. An AVR also improves the generator stability margin. In this paper, the standard IEEE AVR type 1 excitation system model is employed as in Fig. 1 [24].

3.2. DFIG control system

A typical configuration of a DFIG wind turbine technology is shown schematically in Fig. 2. The stator and rotor flux dynamic

Please cite this article in press as: A. Arief, et al., Under voltage load shedding in power systems with wind turbine-driven doubly fed induction generators, Electr. Power Syst. Res. (2012), http://dx.doi.org/10.1016/j.epsr.2012.10.013

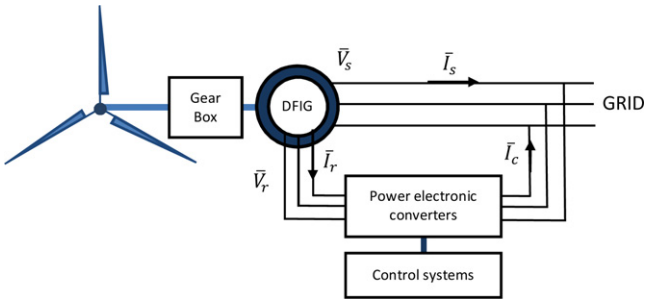

Fig. 2. DFIG wind turbine technology configuration.

are fast compared to the grid dynamic and the control systems of the converter decouple the generator from the grid; hence, the steady-state electrical equations of the DFIG are considered, so that [25]:

$$\upsilon_{ds} = -rsi_{ds} + [(x_s + x_m)i_{qs} + x_m i_{qr}] \quad (1)$$

$$\upsilon_{qs} = -r_s i_{qs} - [(x_s + x_m)i_{ds} + x_m i_{dr}] \quad (2)$$

$$\upsilon_{dr} = -r_R i_{dr} + (1 - \omega_m)[(x_R + x_m)i_{qr} + x_m i_{qs}] \quad (3)$$

$$\upsilon_{qr} = -r_R i_{dr} + (1 - \omega_m)[(x_R + x_m)i_{dr} + x_m i_{ds}] \quad (4)$$

Then, the active and reactive power delivered to the grid become:

$$P = \upsilon_{ds} i_{ds} + \upsilon_{qs} i_{qs} + \upsilon_{dc} i_{dc} + \upsilon_{qc} i_{qc} \quad (5)$$

$$Q = \upsilon_{qs} i_{qs} - \upsilon_{ds} i_{ds} + \upsilon_{qc} i_{qc} - \upsilon_{dc} i_{dc} \quad (6)$$

Since the converter dynamics are fast in comparison with the electromechanical transients, the converter is simplified and modeled as an ideal current source where i_{qr} and i_{dr} are state variables. i_{qr} is employed for the rotor speed control, while i_{dr} is used for voltage control. The schemes of the DFIG rotor speed control and voltage control are given in Figs. 3 and 4, respectively.

Differential equations for the converter currents can be written as:

$$i_{qr} = \left[-\frac{x_s + x_m}{x_m V}\frac{P^*_\omega(\omega_m)}{\omega_m} - i_{qr}\right]\frac{1}{T_\epsilon} \quad (7)$$

$$i_{dr} = K_V(V - V_{ref}) - \frac{V}{x_m} - i_{dr} \quad (8)$$

$P^*_\omega(\omega_m)$ is the power-speed characteristic that optimizes the wind energy capture and is calculated using the rotor speed value.

4. Trajectory sensitivities enhanced UVLS scheme

4.1. Trajectory sensitivity analysis

Trajectory sensitivity analysis is a technique based on linearizing a system surrounding a certain trajectory and employs time domain simulations [26]. This technique computes the sensitivity of the dynamics relating to the constraints [27]. Trajectory sensitivity provides a method of enumerating changes in the system variables in connection with the quick changes of system parameters and initial conditions [28]. The basic methodology of trajectory sensitivity computation of hybrid systems is illustrated in [28], and is discussed as follows.

The systematic representation of a power system which is applicable to voltage stability study is provided by the following differential-algebraic equation (DAE):

$$\dot{x} = f(x, y; \alpha) \quad (9)$$

$$0 = g(x, y; \alpha) \quad (10)$$

where x is the vector of the dynamic state variables; y is the vector of the algebraic state variables such as load bus voltage magnitudes and angles; and α represents system parameters, such as power at the bus.

The trajectories of (9) and (10) illustrate the performance of the dynamic variables x and algebraic variables y, where the flows of x and y can be defined, as:

$$x(t) = \varphi_x(x_0, t, \alpha) \quad (11)$$

$$y(t) = \varphi_y(y_0, t, \alpha) \quad (12)$$

Sensitivities of the flows φ_x and φ_y to the initial conditions and parameter variations can be acquired by forming the Taylor series

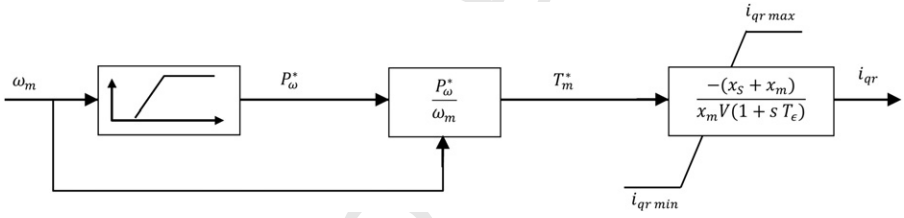

Fig. 3. DFIG rotor speed control [25].

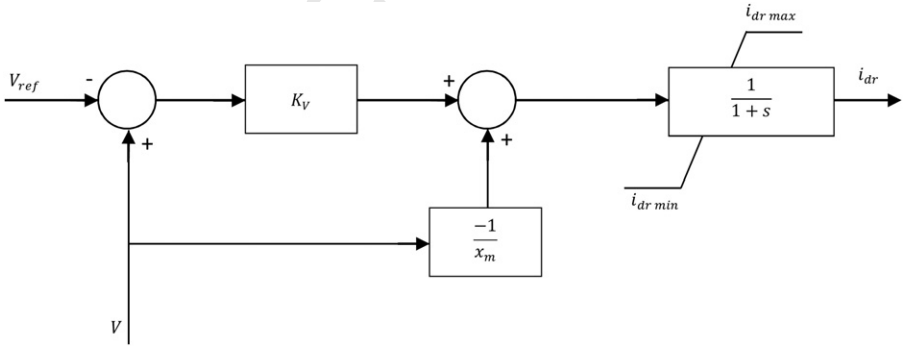

Fig. 4. DFIG voltage control [25].

Please cite this article in press as: A. Arief, et al., Under voltage load shedding in power systems with wind turbine-driven doubly fed induction generators, Electr. Power Syst. Res. (2012), http://dx.doi.org/10.1016/j.epsr.2012.10.013

expansions of the above equations, hence:

$$\Delta x(t) = \Delta\varphi_x(x_0, t, \alpha) = \frac{\partial\varphi_x(x, t, \alpha)}{\partial\alpha}\Delta\alpha = \frac{\partial x(t)}{\partial\alpha}\Delta\alpha \cong x_\alpha(t)\Delta\alpha \tag{13}$$

$$\Delta y(t) = \Delta\varphi_y(y_0, t, \alpha) = \frac{\partial\varphi_y(y_0, t, \alpha)}{\partial\alpha}\Delta\alpha = \frac{\partial y(t)}{\partial\alpha}\Delta\alpha \cong \sim y_\alpha(t)\Delta\alpha \tag{14}$$

An approximation-based numerical method is used to compute the sensitivities x_α and y_α, consequently:

$$x_\alpha = \frac{\partial x}{\partial\alpha} = \frac{\Delta x}{\Delta\alpha} \approx \frac{\varphi_x(x_0, t, \alpha + \Delta\alpha) - \varphi_x(x_0, t, \alpha)}{\Delta\alpha} \tag{15}$$

$$y_\alpha = \frac{\partial y}{\partial\alpha} = \frac{\Delta y}{\Delta\alpha} \approx \frac{\varphi_y(y_0, t, \alpha + \Delta\alpha) - \varphi_y(y_0, t, \alpha)}{\Delta\alpha} \tag{16}$$

The trajectory sensitivities from (14) and (16) are revised to meet the purpose of this study. The bus voltage magnitude and load shedding amount are both parameters represented by y and α correspondingly; hence, the sensitivities of the bus voltage variation after load shedding at any specified bus are computed and can be defined as:

$$\Delta V(t) = \Delta\varphi_V(V_0, t, P) = \frac{\partial\varphi_V(V_0, t, P)}{\partial P}\Delta P = \frac{\partial V(t)}{\partial P}\Delta P \cong V_P(t)\Delta P \tag{17}$$

$$\varphi V_P = \frac{\partial V}{\partial P} = \frac{\Delta V}{\Delta P} \approx \frac{\varphi_V(V_0, t, P + \Delta P) - \varphi_V(V_0, t, P)}{\Delta P} \tag{18}$$

4.2. Trajectory sensitivity factor

In addition, the trajectory sensitivities are performed to find the load shedding location. A trajectory sensitivity factor is formulated to assess the contribution of bus j after load shedding to the system voltage stability. The sensitivities calculated are $[\partial V_i/\partial P_j]$, which inform the rate of change in voltage magnitude at bus i with respect to the load shedding amount variation at bus j. The TSF at bus j is computed by shedding the active power at bus j by a small value, then assessing its impact on voltage magnitudes at all the critical buses along the time domain. The TSF proposed in this work is defined as:

$$TSF_j = TSF_j^{load} + TSF_j^{wind} \tag{19}$$

$$TSF_j^{load} = \sum_{i=1}^{n_k}\left[\sum_{t=0}^{t_s}\left[\frac{\partial V_i^{load}}{\partial P_j}\right]_{t=t_k}\right] \tag{20}$$

$$TSF_j^{wind} = \sum_{i=1}^{n_{wind}}\left[\sum_{t=0}^{t_s}\left[\frac{\partial V_i^{wind}}{\partial P_j}\right]_{t=t_k}\right] \tag{21}$$

$$\partial P_j = \Delta P_j = P_{shed_j}$$

where P_{shed_j}, load shedding amount at bus j; n_k, number of critical buses; n_{wind}, number of aggregated DFIG buses; t_k, time instant; t_s, number of time instants.

There are two components computed here: TSF_j^{load} and TSF_j^{wind}. TSF_j^{load} evaluates the voltage trajectory sensitivities at critical load buses with respect to the load shedding at bus j, whereas TSF_j^{wind} assesses the voltage sensitivities at the wind turbine buses with respect to the load shedding at bus j. The bus with the highest TSF has the largest effect on the voltage stability improvement of the critical buses and hence will be selected as a candidate bus for the location of the UVLS. The flowchart of the proposed trajectory sensitivity-based UVLS is shown in Fig. 5 and can be explained as follows:

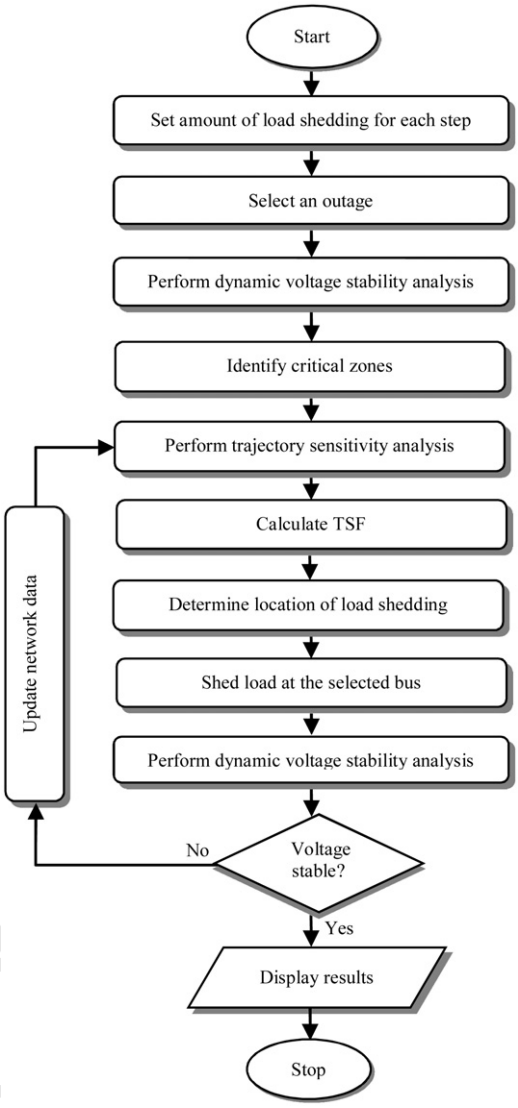

Fig. 5. Flowchart of the trajectory sensitivity-based UVLS design.

Step 1 Set the load shedding amount. In this work, the load shedding amount is set at 5 MW for each iteration.
Step 2 Select an outage.
Step 3 Perform dynamic voltage stability analysis to observe the voltage behavior for all buses.
Step 4 Identify critical zones. This is a zone where buses have a similar pattern of voltage drop.
Step 5 Perform trajectory sensitivity analysis to evaluate the bus voltage trajectory sensitivities.
Step 6 Calculate TSF to assess the contribution of each load bus on improving the voltage stability of the buses at the critical zones. The bus with the highest TSF has the most influence on improving the system voltage magnitude. The location of load shedding is determined based on the highest TSF value.
Step 7 Apply load shedding in the selected bus.
Step 8 Perform dynamic voltage stability analysis to evaluate the system performance after load shedding.

Please cite this article in press as: A. Arief, et al., Under voltage load shedding in power systems with wind turbine-driven doubly fed induction generators, Electr. Power Syst. Res. (2012), http://dx.doi.org/10.1016/j.epsr.2012.10.013

Step 9 If the system is still unstable, then the network data is updated; go to Step 5. This process will be reiterated until the voltage stability constraint is satisfied.

Step 10 If the voltage stability requirement has been fulfilled, then write the results and stop the process.

5. Simulation results

5.1. Without DFIG connected to the system

Q3 The proposed method is implemented at the IEEE 14 bus Reliability Test System (Fig. 6). The system is assumed to be working on a stressed condition. The system load for this study is 511.36 MW, consisting of 50% static load and 50% dynamic motor load. The detail of the load modeling can be seen in [29]. Prior to designing the UVLS scheme, contingency analysis is performed to choose the critical outage. Based on this analysis, the outage between bus 6 and bus 13 is chosen in this study. For the dynamic simulation, a fault is applied between bus 6 and bus 13, and then the fault is cleared by removing the transmission line between bus 6 and bus 13. Firstly, we evaluate the UVLS design without any wind generator. Fig. 7(a) shows the voltage drop after disturbance. There are five critical buses at which the voltage collapses below the stability limit (0.9 pu). They are buses 9, 10, 12, 13 and 14 as shown in Fig. 7(b).

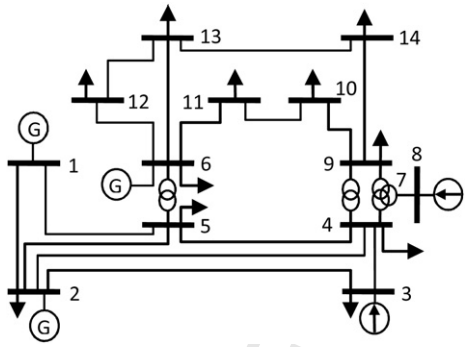

Fig. 6. The test system—IEEE 14 Bus Reliability Test System.

For this simulation, the load-shedding amount for each iteration is set at approximately 1% of the total system load. In this case, we round the amount to 5 MW for each step. The trajectory sensitivity analysis is performed to assess the effect of load shedding of 5 MW at each bus in the critical zone. Fig. 8(a) and (b) illustrates the voltage trajectory sensitivities of critical buses for the first iteration if load shedding is commenced at bus 14 and bus 6, respectively. From both of these figures, it can be concluded that the voltage trajectory sensitivities if load shedding occurs at bus 14 are better than the

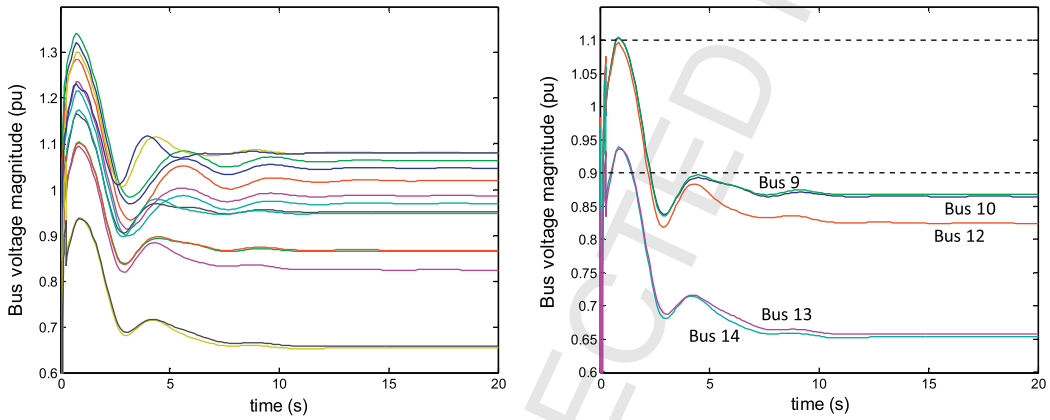

Fig. 7. Voltage drop after outage between bus 6 and bus 13 without DFIG.

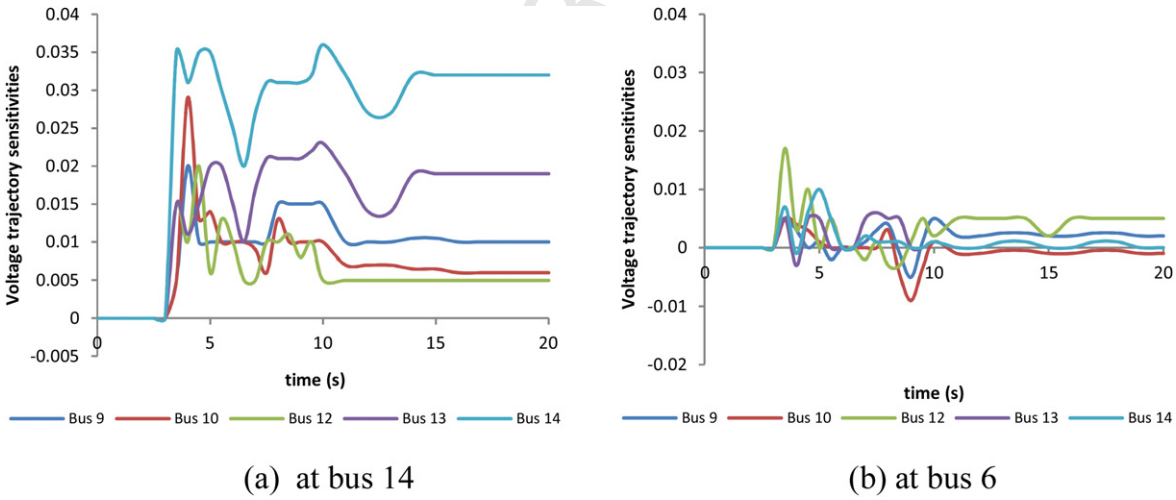

Q4 **Fig. 8.** Bus voltage trajectory sensitivities of critical buses if load shedding is 5 MW. (For interpretation of the references to color in text, the reader is referred to the web version of this article.)

Table 1
TSF calculation for case without DFIG.

$\sum_{t=0}^{t_s}\left[\frac{\partial V_i^{load}}{\partial P_j}\right]_{t=t_k}$		
Bus j / Bus i	14	6
9	0.271	0.037
10	0.223	−0.008
12	0.188	0.083
13	0.432	0.038
14	0.74	0.037
TSF_j^{load}	1.854	0.187

Table 2
TSF values for case without DFIG.

Iteration	TSF value					
	I	II	III	IV	V	VI
Bus number						
2	0.205	0.134	0.110	0.098	0.074	0.026
3	0.211	0.167	0.149	0.106	0.079	0.034
4	0.398	0.302	0.257	0.211	0.086	0.057
5	0.342	0.264	0.216	0.174	0.123	0.089
6	0.187	0.112	0.098	0.077	0.056	0.034
9	0.978	0.849	0.798	0.731	0.674	0.324
10	1.125	1.046	0.987	0.923	0.879	0.585
11	1.302	1.213	1.168	1.092	1.021	0.793
12	1.324	1.265	1.205	1.158	1.115	0.967
13	1.743	1.419	1.367	1.257	1.187	1.076
14	1.854	1.578	1.319	1.296	1.159	1.025

sensitivities at bus 6. Furthermore, TSF is calculated to provide a distinct indication for load shedding location. Here, we only compute the TSF_j^{load} since there are no wind generators yet. In computing the TSF_j^{load} value, we use time interval 0.5 s for the period 0–20 s. Table 1 illustrates the TSF_j^{load} calculation for load shedding at bus 14 and bus 6.

Fig. 9 depicts the TSF value for each load bus at the first iteration. As indicated in the red bar, bus 14 has the highest TSF (1.854). Load shedding of 5 MW is simulated at bus 14 and the system voltage magnitude is re-evaluated. At this stage, the system is still unstable; hence, trajectory sensitivities are performed again to calculate the TSF. For this simulation, this process is repeated six times until the system voltages are stable (above 0.9 pu). The results of the TSF calculation for each iteration and load shedding location based on the highest TSF are presented in Tables 2 and 3, respectively. Hence, the load shedding locations are bus 14 and bus 13 with a load shedding amount at each bus of 15 MW. The results of the

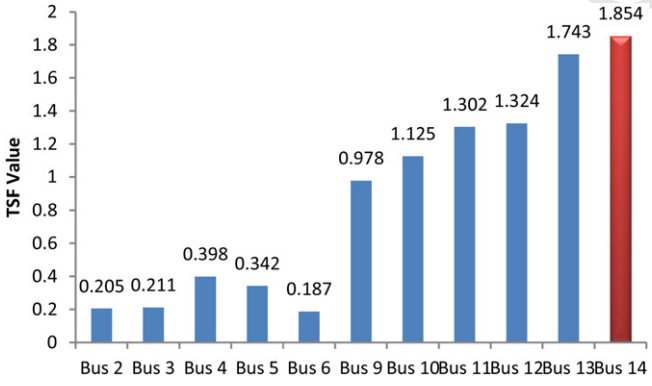

Fig. 9. TSF values at first iteration without DFIG.

Table 3
Load shedding locations for case without DFIG.

Iteration	Load shedding design	
	Location	Amount (MW)
I	Bus 14	5
II	Bus 14	5
III	Bus 13	5
IV	Bus 14	5
V	Bus 13	5
VI	Bus 13	5

Table 4
DFIG parameters.

Power rating	2 MVA
Voltage rating	13.8 kV
Frequency rating	60 Hz
Stator resistance (R_s)	0.01 pu
Stator reactance (X_s)	0.10 pu
Rotor resistance (R_r)	0.01 pu
Rotor reactance (X_r)	0.08 pu
Magnetization reactance (X_m)	3.00 pu
Inertia Constants	3 kWs/kVA

voltage improvement after load shedding of 30 MW at bus 14 and bus 13 can be seen in Fig. 10. It clearly proves that the voltages at all buses improve significantly and that the system stability is recovered.

5.2. With DFIG connected to bus 14

5.2.1. Determination of amount and location of load shedding

To evaluate the UVLS scheme with wind generators, we postulate that aggregated DFIGs are connected to bus 14 with a total accumulative power of 10 MW. The details of the wind generator parameters are shown in Table 4.

Fig. 11(a) portrays the voltage behavior at all buses following a disturbance between bus 6 and bus 13. Specifically, Fig. 11(b) illustrates the voltage drop at the critical buses, of which there are only three (buses 12, 13 and 14).

In order to assess the effect of load shedding on the critical load and DFIG buses, the trajectory sensitivity analysis is carried out. Fig. 12(a) and (b) shows the voltage trajectory sensitivities of critical buses for the first iteration if load shedding is undertaken at bus 14 and bus 13, correspondingly. It is clearly proven that the sensitivities if load shedding occurs in bus 13 are superior than if

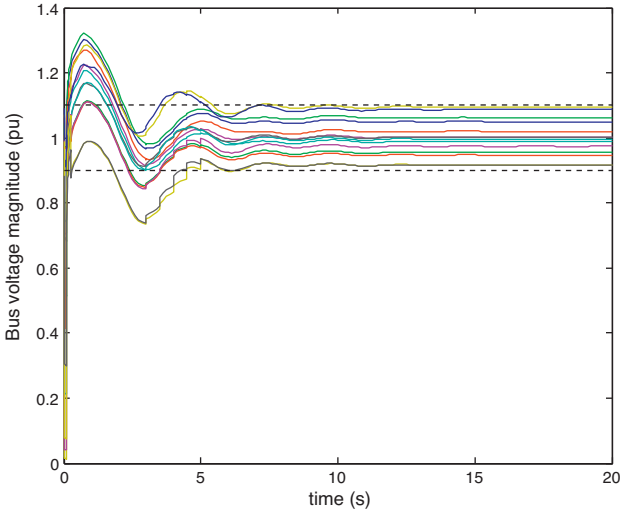

Fig. 10. Voltage profile improvement after load shedding without DFIG.

Please cite this article in press as: A. Arief, et al., Under voltage load shedding in power systems with wind turbine-driven doubly fed induction generators, Electr. Power Syst. Res. (2012), http://dx.doi.org/10.1016/j.epsr.2012.10.013

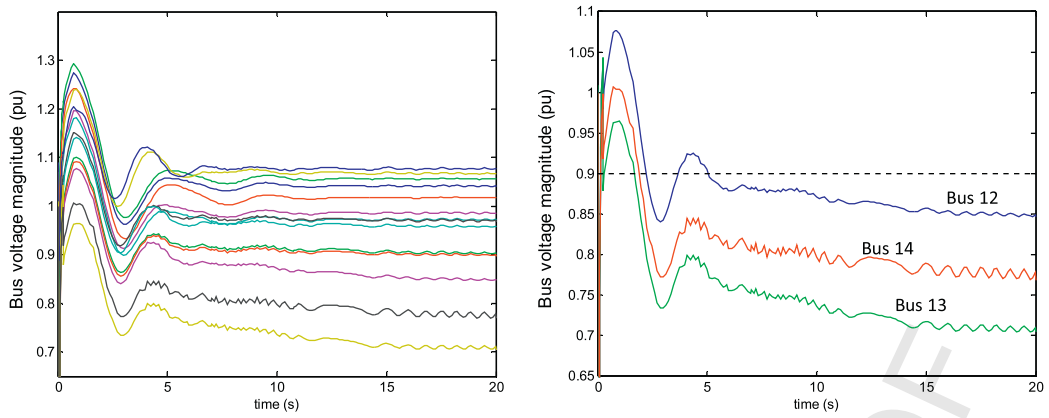

(a) at all load buses (b) at the critical buses

Fig. 11. Voltage drop after outage between bus 6 and bus 13 considering DFIG.

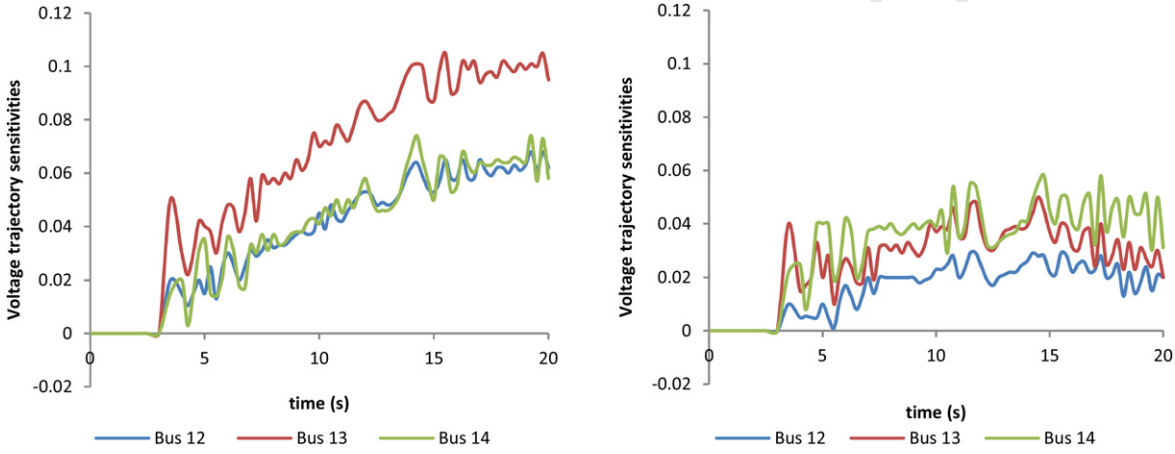

(a) at bus 13 (b) bus 14

Fig. 12. Bus voltage trajectory sensitivities of critical buses if load shedding is 5 MW.

the load shedding occurs at bus 14. In addition, Fig. 13 presents the trajectory sensitivities of the aggregated DFIG voltage if load shedding occurs at buses 14, 13 and 3. It also shows that by load shedding in bus 13, the voltage sensitivities of the DFIG bus are greater than the sensitivities if load shedding occurs at bus 14 or 3. Nevertheless, in order to reach a better quantitative conclusion, the TSF is calculated, consisting of two components: the TSF_j^{load} and the TSF_j^{wind}. Similar to the computation without DFIG, the time interval used is also 0.5 s for the period 0–20 s. The TSF_j calculation for load shedding at buses 14, 13 and 3 is displayed in Table 5.

Fig. 14 conveys the results of the TSF calculation at all load buses. Interestingly, bus 14 no longer has the highest TSF. When the aggregated DFIGs are connected to bus 14, bus 13 now has the largest TSF. Therefore, this bus has the biggest influence on improving the system stability. For this condition, the sensitivity analysis procedure is iterated three times, and the results of this process are expressed in Table 6. After load shedding with a total amount of 15 MW (10 MW

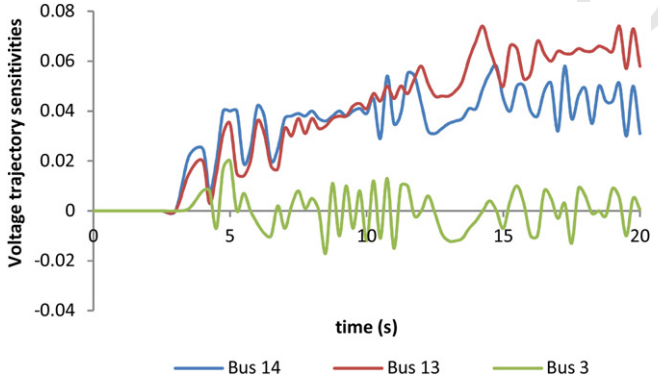

Fig. 13. DFIG voltage trajectory sensitivities with load shedding of 5 MW applied at buses 14, 13 and 3.

Table 5
TSF calculation for case considering DFIG.

Bus j	TSF_j^{load}	TSF_j^{wind}	TSF_j
3	0.0815	0.0365	0.118
13	2.054	0.812	2.866
14	0.851	0.658	1.509

Table 6
Load shedding locations for case considering DFIG.

Iteration	Load shedding design	
	Location	Amount (MW)
I	Bus 13	5
II	Bus 13	5
III	Bus 14	5

Please cite this article in press as: A. Arief, et al., Under voltage load shedding in power systems with wind turbine-driven doubly fed induction generators, Electr. Power Syst. Res. (2012), http://dx.doi.org/10.1016/j.epsr.2012.10.013

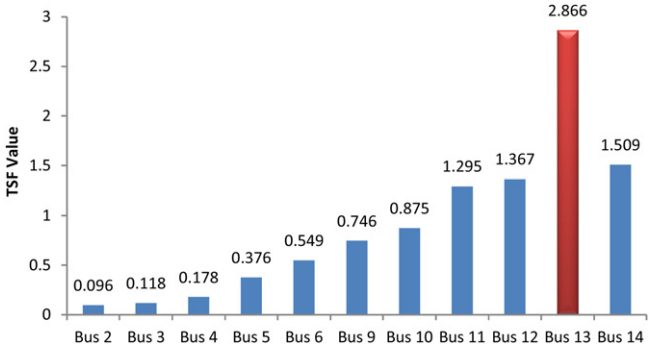

Fig. 14. TSF values at first iteration with DFIG.

at bus 13 and 5 MW at bus 14), the system voltage recovers to its stable condition with the result portrayed in Fig. 15. Table 7 summarizes the comparison of the UVLS design with and without the DFIG connected to the system. It is obvious that, with the integration of wind generators to the system, the UVLS scheme changes and reduces the amount of load to be disengaged from the system. The integration of DG brings positive effects on the voltage profile by providing additional system generation capacity including during outage.

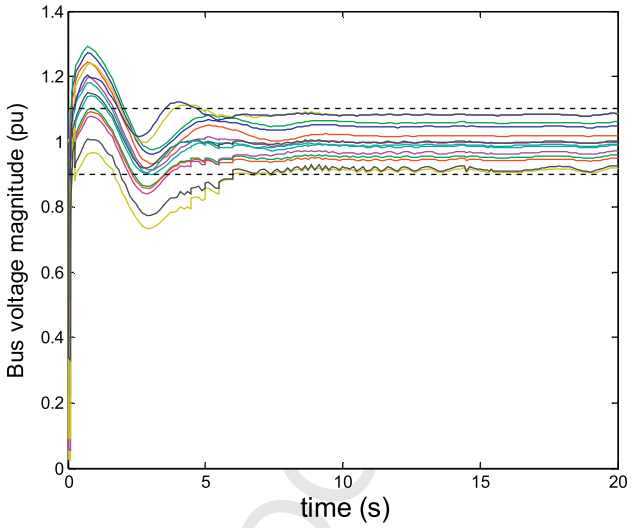

Fig. 15. Voltage profile improvement after load shedding with DFIG.

5.2.2. Analysis of DFIG behavior

Fig. ~~14~~(a–c) demonstrates the DFIG voltage behavior following outage between bus 6 and bus 13 before and after load shedding. Fig. ~~14~~(a) clearly shows that the DFIG voltage decreases to approximately 0.76 pu at $t = 20$ s. In addition, as mentioned in the

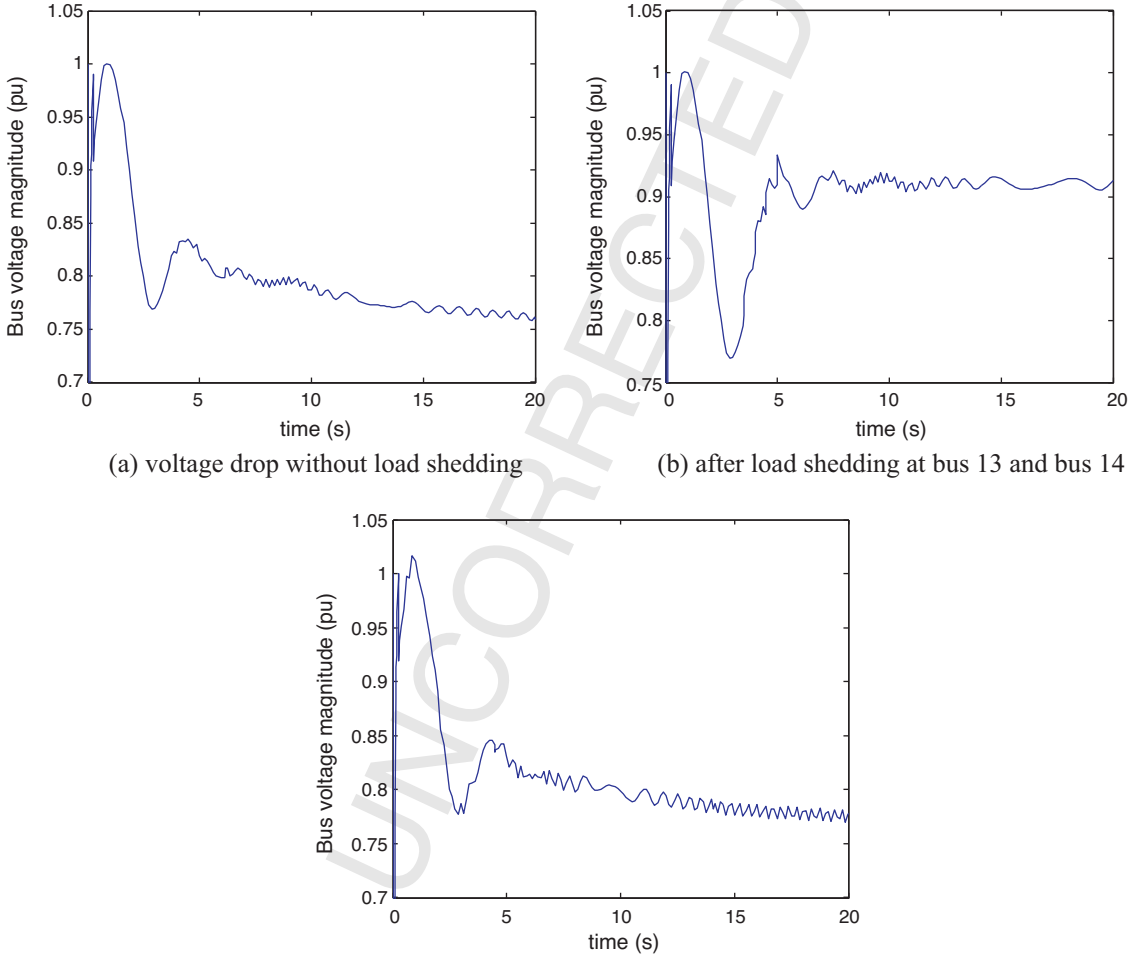

(a) voltage drop without load shedding

(b) after load shedding at bus 13 and bus 14

(c) after load shedding at bus 3

Fig. 16. Voltage behavior at DFIG bus.

Table 7
Comparison load shedding scheme with and without DFIG.

	Load shedding design		
	Location	Amount (MW)	Total (MW)
Without DFIG	Bus 14 Bus 13	15 15	30
With DFIG	Bus 13 Bus 14	10 5	15

introduction, because of this disturbance, the DFIG then supplies asynchornous power to the grid as a result of the excitation converter limitation and its stator that is linked directly to the grid. After load shedding at bus 13 and bus 14 (Fig. ~~14~~1(b)), this asynchronous power still exists even though the DFIG voltage can recover back to its stable condition above 0.9 pu. However, this asynchronous power issue is outside the scope of this work since this work only focuses on determining the amount and location of load shedding to ensure the DFIG voltage can improve. Therefore, another interesting direction to take in further research would be to investigate UVLS design in power systems with DFIG to improve its voltage stability after a disturbance as well as reducing the asynchronous power generated after a disturbance.

Fig. ~~14~~1(c) shows the voltage behavior at the DFIG bus after shedding a load of 15 MW at bus 3. From Table 5, bus 3 has low TSF (0.118) which means it has low impact on improving voltage stability. It shows that load shedding in this bus has no significant impact on improving DFIG voltage stability after being disturbed. The DFIG cannot restore its normal operating condition. Therefore, it is not recommended to shed load at a bus with low TSF ~~(Fig. 16).~~

6. Conclusion

This paper proposes a dynamic analysis-based design of UVLS for stabilizing the system following disturbance and ensuring the system's secure limits are satisfied. The design is based on a trajectory sensitivities technique that calculates the sensitivity of the dynamics relating to the constraints and provides a method of enumerating changes in the system variables in connection with the quick changes of system parameters and initial conditions. In this paper, trajectory sensitivities are employed to determine the minimum amount of the load shedding and to verify the location of the load shedding. The trajectory sensitivity factor provides useful information to find the best location for load shedding. The bus with the highest TSF has the largest effect on enhancing the voltage stability of the critical buses, and hence will be selected as a candidate bus for the location of the UVLS.

This work simulates the system behavior after being perturbed with and without the DFIG. From the simulations, it is seen that the installation of the DFIG can help the demand side management in critical situations by reducing the amount of load to be disconnected from the system. Before installation of the DFIG, the amount of load shedding is 30 MW; whereas, when the DFIG is connected with a total aggregated power of 10 MW, the load shedding amount decreases to 15 MW.

The proposed method provides significant voltage improvement and by using the proposed method, various power system failures after the system has been perturbed can be prevented, including in a power system with wind generators. This method can be applied robustly with or without wind generators and can be applied considering other types of DG as long as the DG unit is modeled accurately.

One problem with the integration of the DFIG is the asynchronous power generated following disturbance. Further research can be undertaken to analyze this issue and investigate how to improve UVLS performance by reducing this asynchronous power.

References

[1] R. Pena, J.C. Clare, G.M. Asher, A doubly fed induction generator using back-to-back PWM converters supplying an isolated load from a variable speed wind turbine, IEE Proceedings: Electric Power Applications 143 (1996) 380–387.
[2] N. Heng, S. Yipeng, Z. Peng, H. Yikang, Improved direct power control of a wind turbine driven doubly fed induction generator during transient grid voltage unbalance, IEEE Transactions on Energy Conversion 26 (2011) 976–986.
[3] E. Vittal, M. O'Malley, A. Keane, A steady-state voltage stability analysis of power systems with high penetrations of wind, IEEE Transactions on Power Systems 25 (2010) 433–442.
[4] V. Akhmatov, P.B. Eriksen, A large wind power system in almost island operation: a Danish case study, IEEE Transactions on Power Systems 22 (2007) 937–943.
[5] M.H. Ali, W. Bin, Comparison of stabilization methods for fixed-speed wind generator systems, IEEE Transactions on Power Delivery 25 (2010) 323–331.
[6] C. Chompooinwai, C. Yingvivatanapong, K. Methaprayoon, L. Wei-Jen, Reactive compensation techniques to improve the ride-through capability of wind turbine during disturbance, IEEE Transactions on Industry Applications 41 (2005) 666–672.
[7] M.J. Hossain, H.R. Pota, M.A. Mahmud, R.A. Ramos, Investigation of the impacts of large-scale wind power penetration on the angle and voltage stability of power systems, IEEE Systems Journal (2011) 1.
[8] H.T. Le, S. Santoso, T.Q. Nguyen, Augmenting wind power penetration and grid voltage stability limits using ESS: application design, sizing, and a case study, IEEE Transactions on Power Systems (2011) 1.
[9] U. Nayeem Rahmat, T. Torbjrn, Variable speed wind turbines for power system stability enhancement, IEEE Transactions on Energy Conversion 22 (2007) 52–60.
[10] E. Vittal, M. O'Malley, A. Keane, Rotor angle stability with high penetrations of wind generation, IEEE Transactions on Power Systems (2011) 1.
[11] W. Yi, X. Lie, Coordinated control of DFIG and FSIG-based wind farms under unbalanced grid conditions, IEEE Transactions on Power Delivery 25 (2010) 367–377.
[12] Z. Peng, H. Yikang, S. Dan, Improved direct power control of a DFIG-based wind turbine during network unbalance, IEEE Transactions on Power Electronics 24 (2009) 2465–2474.
[13] A. Arulampalam, M. Barnes, N. Jenkins, J.B. Ekanayake, Power quality and stability improvement of a wind farm using STATCOM supported with hybrid battery energy storage, IEE Proceedings Generation, Transmission and Distribution 153 (2006) 701–710.
[14] S.K. Salman, A.L.J. Teo, Windmill modelling consideration and factors influencing the stability of a grid-connected wind power-based embedded generator, IEEE Transaction on Power Systems 18 (2003) 793–802.
[15] X. Ding, A.A. Girgis, Optimal load shedding strategy in power systems with distributed generation, in: IEEE Power Engineering Society Winter Meeting, vol. 2, Columbus, OH, January 28–31, 2001, pp. 788–793.
[16] I. Erlich, J. Kretschmann, J. Fortmann, S. Mueller-Engelhardt, H. Wrede, Modeling of wind turbines based on doubly-fed induction generators for power system stability studies, IEEE Transactions on Power Systems 22 (2007) 909–919.
[17] Undervoltage Load Shedding Task Force (UVLSTF) Technical Studies Subcommittee, Undervoltage Load Shedding Guidelines, Western Systems Coordinating Council, July 1999.
[18] S. Imai, Undervoltage load shedding improving security as reasonable measure for extreme contingencies, in: IEEE Power Engineering Society General Meeting, vol. 2, San Francisco, CA, 12–16 June, 2005, pp. 1754–1759.
[19] M. Begovic, D. Fulton, M.R. Gonzalez, J. Goossens, E.A. Guro, R.W. Haas, C.F. Henville, G. Manchur, G.L. Michel, R.C. Pastore, J. Postforoosh, G.L. Schmitt, J.B. Williams, K. Zimmerman, A.A. Burzese, Summary of system protection and voltage stability, IEEE Transactions on Power Delivery 10 (1995) 631–638.
[20] C.J. Mozina, Undervoltage load shedding, in: 60th Annual Conference for Protective Relay Engineers, Texas, USA, 27–29 March, 2007, pp. 16–34.
[21] S.S. Ladhani, W. Rosehart, Under voltage load shedding for voltage stability overview of concepts and principles, in: IEEE Power Engineering Society General Meeting, vol. 2, Denver, CO, 6–10 June, 2004, pp. 1597–1602.
[22] C.M. Affonso, L.C.P. da Silva, F.G.M. Lima, S. Soares, MW and MVar management on supply and demand side for meeting voltage stability margin criteria, IEEE Transactions on Power Systems 19 (2004) 1538–1545.
[23] J.B.X. Devotta, A dynamic model of the synchronous generator excitation control system, IEEE Transactions on Industrial Electronics 34 (1987) 429–432.
[24] IEEE Committee Report, Excitation system models for power system stability studies, IEEE Transactions on Power Apparatus and Systems PAS-100 (1981) 494–509.
[25] F. Milano, Power System Analysis Toolbox, 2005.

Please cite this article in press as: A. Arief, et al., Under voltage load shedding in power systems with wind turbine-driven doubly fed induction generators, Electr. Power Syst. Res. (2012), http://dx.doi.org/10.1016/j.epsr.2012.10.013

[26] K.N. Shubhanga, A.M. Kulkarni, Determination of effectiveness of transient stability controls using reduced number of trajectory sensitivity computations, IEEE Transactions on Power Systems 19 (2004) 473–482.
[27] J. Ma, D. Han, R.-M. He, Z.-Y. Dong, D.J. Hill, Reducing identified parameters of measurement-based composite load model, IEEE Transactions on Power Systems 23 (2008) 76–83.
[28] I.A. Hiskens, M.A. Pai, Trajectory sensitivity analysis of hybrid systems, IEEE Transactions on Circuits and Systems I: Fundamental Theory and Applications 47 (2000) 204–220.
[29] R.M. Rifaat, On composite load modeling for voltage stability and under voltage load shedding, in: IEEE Power Engineering Society General Meeting, vol. 2, Denver, CO, June 7–10, 2004, pp. 1603–1610.

Please cite this article in press as: A. Arief, et al., Under voltage load shedding in power systems with wind turbine-driven doubly fed induction generators, Electr. Power Syst. Res. (2012), http://dx.doi.org/10.1016/j.epsr.2012.10.013